

DEC 27 1976

MAY 10 1977

APR 5 1978

PROPERTY OF U. S. AIR FORCE
AEDC LIBRARY
F40600-75-C-0001

PROPERTY OF U. S. AIR FORCE
AEDC LIBRARY
F40600-75-C-0001

UTRC-R75-911363-15

~~SECRET~~

R75-911363-15

Solution of the Multidimensional
Compressible Navier-Stokes Equations
by a Generalized Implicit Method



DDC
RECEIVED
FEB 17 1976
C

UNITED TECHNOLOGIES RESEARCH CENTER

East Hartford, Connecticut 06108

DISTRIBUTION STATEMENT A
Approved for public release
Distribution Unlimited

Property of U. S. Air Force
AEDC LIBRARY
F40600-75-C-0001

Cy 1

PROPERTY OF U.S. AIR FORCE
AEDC TECHNICAL LIBRARY
ARNOLD AFB, TN 37389

UNITED TECHNOLOGIES RESEARCH CENTER



East Hartford, Connecticut 06108

Property of U. S. Air Force
AEBC LIBRARY
FAC600-75-C-0001

R75-911363-15

Solution of the Multidimensional Compressible Navier-Stokes Equations by a Generalized Implicit Method

Final Report
Contract N00014-72-C-0183

Prepared for
Department of the Navy
Office of Naval Research
Arlington, Virginia

REPORTED BY

W R Briley

W. R. Briley

H M Donald

H. McDonald

H J Gibeling

H. J. Gibeling

APPROVED BY

R E Olson

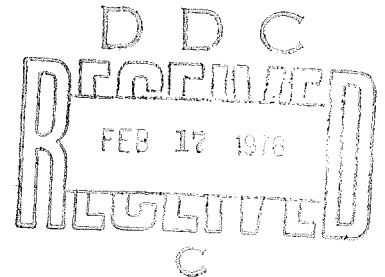
R. E. Olson

DATE January 1976

NO. OF PAGES _____

COPY NO. _____

Approved for Public Release;
Distribution Unlimited



R75-911363-15

Solution of the Multidimensional Compressible
Navier-Stokes Equations by a Generalized
Implicit Method

TABLE OF CONTENTS

	<u>Page</u>
SUMMARY	1
INTRODUCTION	2
Effect of Stability Conditions	2
Steady and Unsteady Applications	3
The Present Method	4
GOVERNING EQUATIONS	6
NUMERICAL METHOD	8
Previous Work	8
Linearization Technique	9
Application of Alternating-Direction Techniques	12
Solution of the Implicit Difference Equations	15
Computing Requirements	18
APPLICATION TO FLOW IN A STRAIGHT DUCT	20
Problem Formulation and Boundary Conditions	20
Stability Tests	21
High Reynolds Number Solutions	23
Convergence Acceleration Tests	26
APPLICATION TO TURBULENT FLOW IN A STRAIGHT DUCT	28
Background	28
Turbulence Model	28
Computed Solutions	36
ACKNOWLEDGEMENT	38
REFERENCES	
FIGURES	
APPENDIX	

R75-911363-15

Solution of the Multidimensional Compressible
Navier-Stokes Equations by a Generalized
Implicit Method

SUMMARY

In an effort to exploit the favorable stability properties of implicit methods and thereby increase computational efficiency by taking large time steps, an implicit finite-difference method for the multidimensional Navier-Stokes equations is presented. The method consists of a generalized implicit scheme which has been linearized by Taylor expansion about the solution at the known time level to produce a set of coupled linear difference equations which are valid for a given time step. To solve these difference equations, the Douglas-Gunn procedure for generating alternating-direction implicit (ADI) schemes as perturbations of fundamental implicit difference schemes is employed. The resulting sequence of narrow block-banded systems can be solved efficiently by standard block-elimination methods. The method is a one-step method, as opposed to a predictor-corrector method, and requires no iteration to compute the solution for a single time step. The use of both second and fourth order spatial differencing is discussed. Test calculations are presented for a three-dimensional application to subsonic flow in a straight duct with rectangular cross section. Stability is demonstrated for time steps which are orders of magnitude larger than the maximum allowable time step for conditionally stable methods as determined by the well known CFL condition. The computational effort per time step is discussed and is very approximately only twice that of most explicit methods. The accuracy of computed solutions is examined by mesh refinement and comparison with other analytical and experimental results. Finally, some test calculations for turbulent flow were made using a simple turbulence model consisting of an eddy viscosity and specified mixing length. The results of these calculations are discussed.

INTRODUCTION

One of the major obstacles to the routine numerical solution of the multidimensional compressible Navier-Stokes equations is the large amount of computer time generally required, and consequently, efficient computational methods are highly desirable in this instance. Most previous methods for solving the compressible Navier-Stokes equations have been based on explicit difference schemes for the unsteady form of the governing equations and are subject to one or more stability restrictions on the size of the time step relative to the spatial mesh size. These stability limits usually correspond to the well known Courant-Friedrichs-Lewy (CFL) condition and, in some schemes, to an additional stability condition arising from viscous terms. In one dimension, the CFL condition is $\Delta t \leq \Delta x / (|u| + c)$, and the viscous stability condition is $\Delta t \leq (\Delta x)^2 / 2\nu$, where Δt is the time step, Δx is the mesh size, u is velocity, c is the speed of sound, and ν is kinematic viscosity. These stability restrictions can lower computational efficiency by imposing a smaller time step than would otherwise be desirable. Thus, a key disadvantage of conditionally stable methods is that the maximum time step is fixed by the spatial mesh size rather than the physical time dependence or the desired temporal accuracy. In contrast to most explicit methods, implicit methods tend to be stable for large time steps and hence offer the prospect of substantial increases in computational efficiency, provided of course that large time steps are acceptable for the physical problem of interest and that the computational effort per time step is competitive with that of explicit methods. In an effort to exploit these potentially favorable stability properties, an efficient implicit method based on alternating-direction differencing techniques was developed and is presented herein.

Effect of Stability Conditions

The potential of implicit methods for increased overall efficiency arises whenever the CFL, viscous, or other stability conditions become restrictive in the sense that the rate of change of physical processes permits a larger step than does the numerical scheme. Since the severity of these stability conditions varies from problem to problem and with the choice of grid size, no single factor can be quoted for overall relative efficiency. Nevertheless, certain guidelines can be established from a consideration of the effect various factors have on the stability conditions. One of the adverse consequences of stability restrictions becomes apparent when a coarse-mesh solution is recomputed with a finer spatial mesh to obtain greater spatial accuracy. Assuming the maximum allowable time-step is taken with a conditionally stable scheme, the time-step must be smaller with the finer mesh even though the physical time dependence is exactly the same. In these same circumstances, implicit methods not subject to stability restrictions can take the same time step with both spatial meshes, and consequently, the computational effort increases only linearly with the number of spatial grid points, as opposed to a quadratic increase

for a CFL-limited calculation and a cubic increase for a viscous-limited calculation. For lower Mach number flows, the CFL condition eventually becomes restrictive regardless of mesh spacing, and thus stable implicit methods are well suited for problems in the low Mach number regime. For all Mach numbers, both the CFL and viscous stability conditions eventually become restrictive for sufficiently small mesh spacing. Implicit methods thus become increasingly attractive when high spatial resolution is necessary and especially when locally refined meshes are used, since the stability limit is usually governed by the smallest mesh spacing in the field. This latter situation is common when more than one length scale is present, as is the case for flows which are largely inviscid but have thin boundary layers requiring a locally refined mesh. Similar statements hold for (time-averaged) turbulent flows with viscous sublayers.

Steady and Unsteady Applications

Although the present method solves the unsteady equations of motion, the most dramatic gains in efficiency are likely to result when computing steady solutions as the asymptotic limit for large time of an unsteady solution. In this instance, there is no need to follow the transient accurately, and large temporal truncation errors can therefore be tolerated and are even desirable in exchange for a reduction in the total number of time steps required to reach steady conditions. Furthermore, various convergence acceleration techniques which take advantage of stability can be employed. For unsteady problems, the need for transient accuracy limits the extent to which the time step can be increased as a result of improved stability, and the relevant question then becomes how the stability limit compares with the time step necessary to follow the transient accurately. This question is difficult to answer with any generality since stability conditions only relate the time step to the spatial mesh size, and they do not directly relate computational time step to the relevant physical time scales of the overall problem.

Although the use of implicit schemes for diffusive terms is generally accepted, it is less clear whether implicit schemes for convective terms have sufficient transient accuracy for unsteady problems (cf. Orszag & Israeli, Ref. 1). Aside from the usual order-of-accuracy error estimates, which are relevant only for sufficiently small step size, indications of the accuracy of a scheme for a given finite step are valuable. Thus, various authors [e.g., Fromm (Ref. 2); Morton (Ref. 3)] have considered the damping and dispersion characteristics of different difference schemes in approximating pure-convection phenomena. For a model problem, Morton (Ref. 3) has pointed out that while the Crank-Nicolson implicit scheme introduces no damping error, certain explicit schemes perform significantly better in terms of phase error per time step as a function of wavelength than does the Crank-Nicolson scheme. Furthermore, it can be shown for this model problem that the phase error of the Crank-Nicolson scheme becomes progressively worse as the explicit stability limit is exceeded, even though the scheme itself remains stable. These findings suggest that implicit schemes for convective terms may not have sufficient

transient accuracy for unsteady problems unless they also satisfy the explicit stability conditions. This argument no doubt has validity in numerous applications wherein the physical time scale of interest is the same as the time scale governing stability. However, the pure-convection model problem does not explore the effects of multiple time scales, boundary conditions, or local regions of high resolution, which are often important in practical applications. Thus, for example, low Mach number unsteady flows can be envisaged wherein the velocity field is insensitive to the detailed behavior of sound waves. Similarly, the unsteadiness may enter through periodic boundary conditions having a time scale longer than that governing stability. Further study in this area would be helpful in assessing the value of implicit schemes in unsteady applications.

The Present Method

Summary

The present method can be briefly outlined as follows: the governing equations are replaced by an implicit time difference approximation, optionally a backward difference or Crank-Nicolson scheme. Terms involving nonlinearities at the implicit time level are linearized by Taylor expansion about the solution at the known time level, and spatial difference approximations are introduced. The result is a system of multidimensional coupled (but linear) difference equations for the dependent variables at the unknown or implicit time level. To solve these difference equations, the Douglas-Gunn (Ref. 4) procedure for generating alternating-direction implicit (ADI) schemes as perturbations of fundamental implicit difference schemes is introduced. This technique leads to systems of coupled linear difference equations having narrow block-banded matrix structures which can be solved efficiently by standard block-elimination methods.

The method centers around the use of a formal linearization technique adapted for the integration of initial-value problems. The linearization technique, which of necessity requires an implicit solution procedure, permits the solution of coupled nonlinear equations in one space dimension (to the requisite degree of accuracy) by a one-step noniterative scheme. Since no iteration is required to compute the solution for a single time step, and since only moderate effort is required for solution of the implicit difference equations, the method is computationally efficient; this efficiency is retained for multidimensional problems by using ADI techniques. The method is also economical in terms of storage, in its present form requiring only two time-levels of storage for each dependent variable. Furthermore, the ADI technique reduces multidimensional problems to sequences of calculations which are one-dimensional in the sense that easily-solved narrow block-banded matrices associated with one-dimensional rows of grid points are produced. Consequently, only these one-dimensional problems require rapid-access storage at any given stage of the solution procedure, and the remaining flow variables can be saved on auxiliary storage devices if desired.

Applicability

Although present attention is focused on the compressible Navier-Stokes equations, the numerical method employed is quite general and is formally derived for systems of governing equations which have the following form:

$$\partial H(\phi) / \partial t = \mathcal{D}(\phi) + S(\phi) \quad (1)$$

where ϕ is a column vector containing ℓ dependent variables, H and S are column vector functions of ϕ , and \mathcal{D} is a column vector whose elements are spatial differential operators which may be multidimensional. The generality of Eq. (1) allows the method to be developed concisely and permits various extensions and modifications (e.g., noncartesian coordinate systems, turbulence models) to be made more or less routinely. It should be emphasized, however, that the Jacobian $\partial H / \partial \phi$ must usually be nonsingular if the ADI techniques as applied to Eq. (1) are to be valid. A necessary condition is that each dependent variable appear in one or more of the governing equations as a time derivative. An exception would occur if for instance, a variable having no time derivative also appeared in only one equation, so that this equation could be decoupled from the remaining equations and solved a posteriori by an alternate method. As a consequence, the present method is not directly applicable to the incompressible Navier-Stokes equations except in one-dimension, where ADI techniques are unnecessary. For example, the velocity-pressure form of the incompressible equations has no time derivative of pressure, whereas the vorticity-stream-function form has no time derivative of stream function. For computing steady solutions, however, the addition of suitable "artificial" time derivatives to the incompressible equations, as was done in Chorin's (Ref. 5) artificial compressibility method, would permit the application of the present method. Alternatively, a low Mach number solution of the compressible equations can be computed.

GOVERNING EQUATIONS

The numerical method is presented for flow in three space dimensions; two-dimensional problems can be treated as a special case. For simplicity, it is assumed that the fluid is a perfect gas with zero bulk viscosity coefficient and constant molecular viscosity, thermal conductivity, and specific heat. The governing equations are nondimensionalized by normalizing dimensional variables with the following reference quantities: distance, L_r ; velocity, U_r ; density, ρ_r ; temperature; T_r ; time, L_r/U_r ; enthalpy U_r^2 ; and pressure, $\rho_r U_r^2/g$, where g is the gravitational constant. This normalization leads to the following nondimensional parameters: Mach number, M ; Reynolds number, Re ; Prandtl number, Pr ; and specific heat ratio, γ . These parameters are defined by

$$M = U_r / c, \quad Re = \rho_r U_r L_r / \mu, \quad Pr = c_p \mu / k, \quad \gamma = c_p / c_v \quad (2a-d)$$

where μ is the molecular viscosity, k is thermal conductivity, and c_p and c_v are the specific heats at constant pressure and volume. The reference speed of sound, c , is defined by $c^2 = \gamma g R T_r$, where R is the gas constant.

With the exception of the energy equation, the equations are written in the so-called conservation form. The foregoing assumptions are convenient but not essential; the treatment of alternate forms of the equations, arbitrary equation of state, and variable fluid properties is relatively straightforward. With the stated assumptions, the Navier-Stokes equations can be written for Cartesian coordinates (x,y,z) as follows: the continuity equation is

$$\partial \rho / \partial t = \partial(-\rho u) / \partial x + \partial(-\rho v) / \partial y + \partial(-\rho w) / \partial z \quad (3a)$$

The momentum equations are represented by

$$\partial(\rho \tilde{u}) / \partial t = \partial(-\rho u \tilde{u}) / \partial x + \partial(-\rho v \tilde{u}) / \partial y + \partial(-\rho w \tilde{u}) / \partial z - \partial p / \partial \tilde{x} + \tilde{F} \quad (3b)$$

The energy equation is

$$\begin{aligned} \frac{\partial \rho T}{\partial t} = & \frac{\partial}{\partial x} \left(-\rho u T + \frac{\gamma}{Re Pr} \frac{\partial T}{\partial x} \right) + \frac{\partial}{\partial y} \left(-\rho v T + \frac{\gamma}{Re Pr} \frac{\partial T}{\partial y} \right) + \\ & \frac{\partial}{\partial z} \left(-\rho w T + \frac{\gamma}{Re Pr} \frac{\partial T}{\partial z} \right) + \gamma(\gamma-1)M^2 \left[\frac{1}{Re} \Phi - \rho(\nabla \cdot \mathbf{u}) \right] \end{aligned} \quad (3c)$$

In Eqs. (3), u , v , and w are the x , y and z components of the velocity vector, U ; ρ is density; T is temperature; p is pressure; t is time, and ∇ is the gradient operator. The symbols \tilde{u} , \tilde{x} denote u , x ; v , y ; w , z , respectively, for the x , y , and z momentum equations.

The force due to viscous stress, \tilde{F} , is given by

$$\tilde{F} = \frac{1}{Re} \left[\partial^2 \tilde{u} / \partial x^2 + \partial^2 \tilde{u} / \partial y^2 + \partial^2 \tilde{u} / \partial z^2 + \frac{1}{3} \partial(\nabla \cdot U) / \partial \tilde{x} \right] \quad (4)$$

The dissipation function, Φ , is given by

$$\Phi = 2 \left[\left(\frac{\partial u}{\partial x} \right)^2 + \left(\frac{\partial v}{\partial y} \right)^2 + \left(\frac{\partial w}{\partial z} \right)^2 \right] + \left(\frac{\partial u}{\partial y} + \frac{\partial v}{\partial x} \right)^2 + \left(\frac{\partial v}{\partial z} + \frac{\partial w}{\partial y} \right)^2 + \left(\frac{\partial u}{\partial z} + \frac{\partial w}{\partial x} \right)^2 - \frac{2}{3} (\nabla \cdot U)^2 \quad (5)$$

The pressure can be eliminated as a dependent variable by means of the equation of state for a perfect gas,

$$p = \rho T / \gamma M^2 \quad (6)$$

The continuity, momentum and energy equations thus constitute a system of five equations in the dependent variables ρ , u , v , w , and T . The definition of total enthalpy E is

$$E = T / (\gamma - 1) M^2 + q^2 / 2 \quad (7)$$

where $q^2 = u^2 + v^2 + w^2$. In numerous problems of interest, it can be assumed that the total enthalpy is a constant E_0 provided there is no heat addition. This assumption is reasonable for inviscid flow regions with or without shocks and for boundary layers on adiabatic walls provided the Prandtl number is unity. In this circumstance, Eqs. (6-7) can be combined to produce an adiabatic equation of state,

$$\rho = \rho(E_0 - q^2 / 2) (\gamma - 1) / \gamma \quad (8)$$

If pressure is eliminated in the momentum equations by means of (8), then solution of the energy equation (3c) is unnecessary, and a significant reduction in computational effort is effected. The temperature field is then determined a posteriori from Eq. (7). This simplification, although convenient and available as an option, was not used for any of the calculations presented here for laminar flow.

NUMERICAL METHOD

Previous Work

Although several methods based on implicit schemes have been developed for incompressible flows (e.g., Pearson, Ref. 6; Chorin, Ref. 7), most previous methods for the compressible Navier-Stokes equations have employed explicit schemes. Nevertheless, a semi-implicit method has been developed by Harlow and Amsden (Ref. 8) for use over the entire spectrum of Mach numbers from incompressible to hypersonic. However, the Harlow-Amsden method treats viscous terms explicitly and, unlike alternating-direction methods, requires the solution of multidimensional implicit difference equations, which tends to be time consuming. In an independent investigation, Baum and Ndefo (Ref. 9) developed a two-dimensional implicit method which is patterned after the original Peaceman-Rachford (Ref. 10) ADI technique. Perhaps the most significant difference between the Baum-Ndefo and present methods is that the Baum-Ndefo method employs iterative techniques, solving nonlinear difference equations as a sequence of linear equations, whereas in the present method, the difference equations are linearized about the solution at the previous time step and solved without iteration. In principle, the solution of nonlinear difference equations is of course attractive, as this removes any limitations which might arise from the linearization process. It is, however, a time-consuming process to solve the nonlinear difference equations, and as far as temporal accuracy is concerned, the additional computational effort required by the solution of nonlinear difference equations might be as well spent by reducing the time step and proceeding with a satisfactory linearization (McDonald & Briley, Ref. 11).

On the other hand, if a steady solution is the only objective, then temporal accuracy is of little concern, and a stable method requiring minimal computational effort per time step (the present objective) is attractive. The topic of nonlinear truncation errors is discussed further by McDonald and Briley (Ref. 11).

The present numerical method was developed for the Navier-Stokes equations by Briley and McDonald (Ref. 12) and for steady supersonic flows by McDonald and Briley (Ref. 11). Here the method is formalized for mixed parabolic-hyperbolic systems having the form of Eq. (1), and is applied to the Navier-Stokes equations.

Recently, Beam and Warming (Ref. 13) have specialized this same linearization procedure to equations in conservation-law form, with emphasis on the inviscid Euler equations. Beam and Warming also employed compact spatial differencing techniques analogous to those discussed by Mitchell (Ref. 14, p. 51) but in more general circumstances. Although highly effective as applied by Beam and Warming to conservation laws, the compact spatial differencing appears to lose its advantage in computational efficiency over more conventional differencing techniques, whenever both first and second-order derivatives are present. This point will be

discussed subsequently. Beam and Warming also suggested valuable techniques for use in computing flows containing shocks.

Linearization Technique

Background

A number of techniques have been used for implicit solution of the following first-order nonlinear scalar equation in one dependent variable $\phi(x,t)$:

$$\partial\phi/\partial t = F(\phi) \partial G(\phi)/\partial x \quad (9)$$

Special cases of Eq. (9) include the conservation form if $F(\phi) = 1$, and quasilinear form if $G(\phi) = \phi$. Previous implicit methods for Eq. (9) which employ nonlinear difference equations and also methods based on two-step predictor-corrector schemes are discussed by Ames (Ref. 15, p. 82) and von Rosenberg (Ref. 16, p. 56). One such method is to difference nonlinear terms directly at the implicit time level to obtain nonlinear implicit difference equations; these are then solved iteratively by a procedure such as Newton's method. Although otherwise attractive, there may be difficulty with convergence in the iterative solution of the nonlinear difference equations, and some efficiency is sacrificed by the need for iteration. An implicit predictor-corrector technique has been devised by Douglas and Jones (Ref. 17) which is applicable to the quasilinear case ($G = \phi$) of Eq. (9). The first step of their procedure is to linearize the equation by evaluating the nonlinear coefficient as $F(\phi^n)$ and to predict values of $\phi^{n+\frac{1}{2}}$ using either the backward difference or the Crank-Nicolson scheme. Values for ϕ^{n+1} are then computed in a similar manner using $F(\phi^{n+\frac{1}{2}})$ and the Crank-Nicolson scheme. Gourlay and Morris (Ref. 18) have also proposed implicit predictor-corrector techniques which can be applied to Eq. (9). In the conservative case ($F=1$), their technique is to define $\hat{G}(\phi)$ by the relation $G(\phi) = \phi \hat{G}(\phi)$ when such a definition exists, and to evaluate $\hat{G}(\phi^{n+1})$ using values for ϕ^{n+1} computed by an explicit predictor scheme. With \hat{G} thereby known at the implicit time level, the equation can be treated as linear, and corrected values of ϕ^{n+1} are computed by the Crank-Nicolson scheme.

A technique is described here for deriving linear implicit difference approximations for nonlinear differential equations. The technique is based on an expansion of nonlinear implicit terms about the solution at the known time level, t^n , and leads to a one-step, two-level scheme which, being linear in unknown (implicit) quantities, can be solved efficiently without iteration. This idea was applied by Richtmyer and Morton (Ref. 19, p. 203) to a scalar nonlinear diffusion equation. Here, the technique is developed for problems governed by ℓ nonlinear equations in ℓ dependent variables which are functions of time and space coordinates. Attention is restricted to nonlinear systems having the form of Eq. (1).

The solution domain is discretized by grid points having equal spacings, Δx , Δy , and Δz , in the x , y , and z directions, respectively, and an arbitrary time step, Δt . Provisions for nonuniform grid spacing will be introduced subsequently. The subscripts i, j, k and superscript n are grid point indices associated with x, y, z , and t , respectively, and thus $\phi_{i,j,k}^n$ denotes $\phi(x_i, y_j, z_k, t^n)$. It is assumed that the solution is known at the n level, t^n , and is desired at the $(n+1)$ level, t^{n+1} . At the risk of an occasional ambiguity, one or more of the subscripts is frequently omitted, so that ϕ^n is equivalent to $\phi_{i,j,k}^n$.

Linearized Difference Scheme

The linearized difference approximation is derived from the following implicit time-difference replacement of Eq. (1):

$$(H^{n+1} - H^n) / \Delta t = \beta [\mathcal{D}(\phi^{n+1}) + S^{n+1}] + (1 - \beta) [\mathcal{D}(\phi^n) + S^n] \quad (10)$$

where, for example, $H^{n+1} \equiv H(\phi^{n+1})$. The form of D and the spatial differencing are as yet unspecified. A parameter β ($0 \leq \beta \leq 1$) has been introduced so as to permit a variable centering of the scheme in time. Equation (10) produces a backward difference formulation for $\beta = 1$ and a Crank-Nicolson formulation for $\beta = 1/2$. Unconditional stability is anticipated for $\beta > 1/2$.

The linearization is performed by a two-step process of expansion about the known time level t^n and subsequent approximation of the quantity $(\partial/\partial t)^n \Delta t$, which arises from chain rule differentiation, by $(\phi^{n+1} - \phi^n)$. The result is

$$H^{n+1} = H^n + (\partial H / \partial \phi)^n (\phi^{n+1} - \phi^n) + O(\Delta t)^2 \quad (11a)$$

$$S^{n+1} = S^n + (\partial S / \partial \phi)^n (\phi^{n+1} - \phi^n) + O(\Delta t)^2 \quad (11b)$$

$$\mathcal{D}(\phi^{n+1}) = \mathcal{D}(\phi^n) + (\partial \mathcal{D} / \partial \phi)^n (\phi^{n+1} - \phi^n) + O(\Delta t)^2 \quad (11c)$$

The matrices $\partial H / \partial \phi$ and $\partial S / \partial \phi$ are standard Jacobians whose elements are defined, for example, by $(\partial H / \partial \phi)_{qr} \equiv \partial H_q / \partial \phi_r$. The operator elements of the matrix $\partial \mathcal{D} / \partial \phi$ are similarly ordered, i.e., $(\partial \mathcal{D} / \partial \phi)_{qr} \equiv \partial \mathcal{D}_q / \partial \phi_r$; however, the intended meaning of the operator elements requires some clarification. For the q th row, the operation $(\partial \mathcal{D}_q / \partial \phi)^n (\phi^{n+1} - \phi^n)$ is understood to mean that $\{\partial / \partial t \mathcal{D}_q[\phi(x, y, z, t)]\}^n \Delta t$ is computed and that all occurrences of $(\partial \phi_r / \partial t)^n$ arising from chain rule differentiation are replaced by $(\phi_r^{n+1} - \phi_r^n) / \Delta t$.

After linearization as in Eqs. (11), Eq. (10) becomes the following linear implicit time-differenced scheme:

$$(\partial H^n / \partial \phi)(\phi^{n+1} - \phi^n) / \Delta t = \mathcal{D}(\phi^n) + S^n + \beta (\partial \mathcal{D} / \partial \phi + \partial S^n / \partial \phi)(\phi^{n+1} - \phi^n) \quad (12)$$

Although H^{n+1} is linearized to second order in Eq. (11a), the division by Δt in Eq. (10) introduces an error term of order Δt . A technique for maintaining formal second-order accuracy in the presence of nonlinear time derivatives is discussed by McDonald and Briley (Ref. 11), however a three-level scheme results. Second-order temporal accuracy can also be obtained (for $\beta = 1/2$) by a change in dependent variable to $\phi \equiv H(\phi)$, provided this is convenient, since the nonlinear time derivative is then eliminated. The temporal accuracy is independent of the spatial accuracy.

On examination, it can be seen that Eq. (12) is linear in the quantity $(\phi^{n+1} - \phi^n)$ and that all other quantities are either known or evaluated at the n level. Computationally, it is convenient to solve Eq. (12) for $(\phi^{n+1} - \phi^n)$ rather than ϕ^{n+1} . This both simplifies Eq. (12) and reduces roundoff errors, since it is presumably better to compute a small $O(\Delta t)$ change in an $O(1)$ quantity than the quantity itself. To simplify the notation, a new dependent variable ψ defined by

$$\psi \equiv \phi - \phi^n \quad (13)$$

is introduced, and thus $\psi^{n+1} = \phi^{n+1} - \phi^n$, and $\psi^n = 0$. It is also convenient to rewrite Eq. (12) in the following simplified form:

$$(A + \Delta t \mathcal{L}) \psi^{n+1} = \Delta t [\mathcal{D}(\phi^n) + S^n] \quad (14a)$$

where the following symbols have been introduced to simplify the notation:

$$A \equiv \partial H^n / \partial \phi - \beta \Delta t (\partial S^n / \partial \phi) \quad (14b)$$

$$\mathcal{L} \equiv -\beta (\partial \mathcal{D} / \partial \phi) \quad (14c)$$

It is noted that $\mathcal{L}(\psi)$ is a linear transformation and thus $\mathcal{L}(0) = 0$. Furthermore, if $\mathcal{D}(\phi)$ is linear, then $\mathcal{L}(\psi) = -\beta \mathcal{D}(\psi)$.

Spatial differencing of Eq. (14a) is accomplished simply by replacing derivative operators such as $\partial/\partial x$, $\partial^2/\partial x^2$ by corresponding finite difference operators, D_x , D_x^2 . Henceforth, it is assumed that \mathcal{D} and \mathcal{L} have been discretized in this manner, unless otherwise noted.

In practice, difference schemes generated by the foregoing procedures are often quite simple. For example, the continuity equation (3a) becomes

$$(\rho^{n+1} - \rho^n) = -\beta \Delta t \sum_{(\tilde{u}, \tilde{x})} D_{\tilde{x}} \left[\rho^{n+1} \tilde{u}^n + \rho^n \tilde{u}^{n+1} + \left(\frac{1-2\beta}{\beta} \right) \rho^n \tilde{u}^n \right] \quad (15)$$

which couples ρ^{n+1} and \tilde{u}^{n+1} .

Discussion

Before proceeding, some general observations seem appropriate. The foregoing linearization technique assumes only Taylor expandability, an assumption already implicit in the use of a finite difference method. The governing equations and boundary conditions are addressed directly as a system of coupled nonlinear equations which collectively determine the solution. The approach thus seems more natural than that of making ad hoc linearization and decoupling approximations, as is often done in applying implicit schemes to coupled and/or nonlinear partial differential equations. With the present approach, it is not necessary to associate each governing equation and boundary condition with a particular dependent variable (e.g., assumed u is governed by the x momentum equation, ρ by continuity, etc.) and then to identify various "nonlinear coefficients" and "coupling terms" which must then be treated by lagging, predictor-corrector techniques, or iteration. The Taylor expansion procedure is analogous to that used in the generalized Newton-Raphson or quasilinearization methods for iterative solution of nonlinear systems by expansion about a known current guess at the solution (e.g., Bellman & Kalaba, Ref. 20). However, the concept of expanding about the previous time level has apparently not been employed to produce a noniterative implicit time-dependent scheme for coupled equations, wherein nonlinear terms are approximated to a level of accuracy commensurate with that of the time differencing. The linearization technique also permits the implicit treatment of coupled nonlinear boundary conditions, such as stagnation pressure and enthalpy at subsonic inlet boundaries, and in practice, this latter feature was found to be crucial to the stability of the overall method.

Application of Alternating-Direction Techniques

Solution of Eq. (14a) is accomplished by application of an alternating-direction implicit (ADI) technique for parabolic-hyperbolic equations. The original ADI method was introduced by Peaceman and Rachford (Ref. 10) and Douglas (Ref. 21); however, the alternating-direction concept has since been expanded and generalized. A discussion of various alternating-direction techniques is given by Mitchell (Ref. 14) and Yanenko (Ref. 22).

The present technique is simply an application of the very general procedure developed by Douglas and Gunn (Ref. 4) for generating ADI schemes as perturbations of fundamental implicit difference schemes such as the backward-difference or Crank-Nicolson schemes.

For the present, it will be assumed that $\mathcal{D}(\phi)$ contains derivatives of first and second order with respect to x , y , and z , but no mixed derivatives. In this case, \mathcal{D} can be split into three operators, \mathcal{D}_x , \mathcal{D}_y , \mathcal{D}_z associated with the x , y , and z coordinates and each having the functional form $\mathcal{D}_{\tilde{x}} = a(\phi, \partial/\partial\tilde{x}, \partial^2/\partial\tilde{x}^2)$ for a typical coordinate \tilde{x} . Equation (14a) then becomes

$$[A + \Delta t(\mathcal{L}_x + \mathcal{L}_y + \mathcal{L}_z)]\psi^{n+1} = \Delta t[(\mathcal{D}_x + \mathcal{D}_y + \mathcal{D}_z)\phi^n + s^n] \quad (16)$$

Recalling that $\mathcal{L}(\psi^n) = 0$, the Douglas-Gunn representation of Eq. (16) can be written as the following three-step solution procedure:

$$(A + \Delta t \mathcal{L}_x)\psi^* = \Delta t[(\mathcal{D}_x + \mathcal{D}_y + \mathcal{D}_z)\phi^n + s^n] \quad (17a)$$

$$(A + \Delta t \mathcal{L}_y)\psi^{**} = A\psi^* \quad (17b)$$

$$(A + \Delta t \mathcal{L}_z)\psi^{n+1} = A\psi^{**} \quad (17c)$$

where ψ^* and ψ^{**} are intermediate solutions. It will be shown subsequently that each of Eqs. (17) can be written in narrow block-banded matrix form and solved by efficient block-elimination methods. If ψ^* and ψ^{**} are eliminated, Eqs. (17) become

$$(A + \Delta t \mathcal{L}_x)A^{-1}(A + \Delta t \mathcal{L}_y)A^{-1}(A + \Delta t \mathcal{L}_z)\psi^{n+1} = \Delta t[(\mathcal{D}_x + \mathcal{D}_y + \mathcal{D}_z)\phi^n + s^n] \quad (18)$$

If the multiplication on the left-hand side of Eq. (18) is performed, it becomes apparent that Eq. (18) approximates Eq. (16) to order $(\Delta t)^2$. Although the stability of Eqs. (17) has not been established in circumstances sufficiently general to encompass the Navier-Stokes equations, it is often suggested (e.g., Richtmyer & Morton, Ref. 19, p. 215) that the scheme is stable and accurate under conditions more general than those for which rigorous proofs are available. This latter notion is adopted here as a working hypothesis supported by favorable results obtained in actual computations.

A major attraction of the Douglas-Gunn scheme is that the intermediate solutions ψ^* and ψ^{**} are consistent approximations to ψ^{n+1} . Furthermore, for steady solutions, $\psi^n = \psi^* = \psi^{**} = \psi^{n+1}$ independent of Δt . Thus, physical boundary conditions for ψ^{n+1} can be used in the intermediate steps without a serious loss in accuracy and with no loss for steady solutions. In this respect, the Douglas-Gunn scheme appears to have an advantage over locally one-dimensional (LOD) or "splitting" schemes, and other schemes whose intermediate steps do not satisfy the consistency condition. The lack of consistency in the intermediate steps complicates the treatment of boundary conditions and, according to Yanenko (Ref. 22, p. 33), does not permit the use of asymptotically large time steps. It is not clear that this advantage of the Douglas-Gunn scheme would always outweigh other benefits which might be derived from an alternative scheme. However, since the ADI scheme can be viewed

as an approximate technique for solving the fundamental difference scheme, Eq. (14a), alternate ADI schemes can readily be used within the present formulation.

It is worth noting that the operator \mathfrak{D} can be split into any number of components which need not be associated with a particular coordinate direction. As pointed out by Douglas and Gunn (Ref. 4), the criterion for identifying sub-operators is that the associated matrices be "easily solved" (i.e. narrow-banded). Thus, mixed derivatives can be treated implicitly within the ADI framework, although this would increase the number of intermediate steps and thereby complicate the solution procedure. Finally, only minor changes are introduced if, in the foregoing development of the numerical method, H , \mathfrak{D} , and S are functions of the spatial coordinates and time, as well as ϕ .

Solution of the Implicit Difference Equations

Second-Order Spatial Differences

Since each of Eqs. (17) is implicit in only one coordinate direction, the solution procedure can be discussed with reference to a one-dimensional problem. For simplicity, it is sufficient to consider Eq. (17a) with $\mathcal{D}_y, \mathcal{D}_z \equiv 0$. For the moment, attention is focused on the following three-point difference formulas:

$$D_{\tilde{x}} \phi \equiv [\alpha \Delta_- + (1-\alpha) \Delta_+] \phi / \Delta \tilde{x} = (\partial \phi / \partial \tilde{x})_i + o[\Delta \tilde{x}^2 + (\alpha - 1/2) \Delta \tilde{x}] \quad (19a)$$

$$D_{\tilde{x}}^2 \phi \equiv (\Delta_+ \Delta_-) \phi / (\Delta \tilde{x})^2 = (\partial^2 \phi / \partial \tilde{x}^2)_i + o(\Delta \tilde{x}^2) \quad (19b)$$

for a typical coordinate \tilde{x} . Here, $\Delta_- \equiv \phi_i - \phi_{i-1}$, $\Delta_+ \equiv \phi_{i+1} - \phi_i$, and a parameter α has been introduced ($0 \leq \alpha \leq 1$) so as to permit continuous variation from backward to forward differences. The standard central difference formula is recovered for $\alpha = \frac{1}{2}$ and was used for all solutions reported here.

As an example, suppose that the q th component of \mathcal{D}_x has the form

$$\mathcal{D}_{xq}(\phi) = F_{1q}^T(\phi) \frac{\partial}{\partial x} G_{1q}(\phi) + F_{2q}^T(\phi) \frac{\partial^2}{\partial x^2} G_{2q}(\phi) \quad (20)$$

where F and G are column vector functions having the same but an arbitrary number of components; F^T denotes the transpose of F . The form of Eq. (20) permits governing equations having any number of first and second derivative terms. Then,

$$\begin{aligned} (\partial \mathcal{D}_{xq} / \partial \phi)(\phi^{n+1} - \phi^n) &\equiv F_{1q}^T \frac{\partial}{\partial x} \frac{\partial G_{1q}}{\partial \phi} (\phi^{n+1} - \phi^n) + \frac{\partial F_{1q}^T}{\partial \phi} (\phi^{n+1} - \phi^n) \frac{\partial G_{1q}}{\partial x} \\ &+ F_{2q}^T \frac{\partial^2}{\partial x^2} \frac{\partial G_{2q}}{\partial \phi} (\phi^{n+1} - \phi^n) + \frac{\partial F_{2q}^T}{\partial \phi} (\phi^{n+1} - \phi^n) \frac{\partial^2 G_{2q}}{\partial x^2} \end{aligned} \quad (21)$$

It is now possible to describe the solution procedure for Eq. (17a) for the one-dimensional case with \mathcal{D}_x given by Eq. (20) and difference formulas given by Eq. (19). Because of the spatial difference operators, D_x and D_x^2 , Eq. (17a) contains ψ_{i-1}^* , ψ_i^* , and ψ_{i+1}^* ; consequently, the system of linear equations generated by writing Eq. (17a) at successive grid points x_i can be written in block-tridiagonal form (simple tridiagonal for scalar equations, $\ell = 1$). The block-tridiagonal

matrix structure emerges from rewriting Eq. (17a) as

$$a_i^n \psi_{i-1}^* + b_i^n \psi_i^* + c_i^n \psi_{i+1}^* = d_i^n \quad (22)$$

where a, b, c are square matrices and d is a column vector, each containing only n-level quantities. The qth component of d and qth row-components of a, b, c are given by

$$(a_i^n)_q = \left[(\partial F_{1q}^T / \partial \phi)_i^n (G_{1q})_{i-1}^n + (F_{1q}^+)_i^n (2G_{1q} / 2\phi)_{i-1}^n \right] \alpha / \Delta x \\ - \left[(\partial F_{2q}^T / \partial \phi)_i^n (G_{2q})_{i-1}^n + (F_{2q}^T)_i^n (\partial G_{2q} / \partial \phi)_{i-1}^n \right] / (\Delta x)^2 \quad (23a)$$

$$(b_i^n)_q = (\partial H_q / \partial \phi)_i^n / \beta \Delta t - (\partial S_q / \partial \phi)_i^n \\ + \left[(\partial F_{1q}^T / \partial \phi)_i^n (G_{1q})_i^n + (F_{1q}^T)_i^n (\partial G_{1q} / \partial \phi)_i^n \right] (1-2\alpha) / \Delta x \\ + 2 \left[(\partial F_{2q}^T / \partial \phi)_i^n (G_{2q})_i^n + (F_{2q}^T)_i^n (\partial G_{2q} / \partial \phi)_i^n \right] / (\Delta x)^2 \quad (23b)$$

$$(c_i^n)_q = \left[(\partial F_{1q}^T / \partial \phi)_i^n (G_{1q})_{i+1}^n + (F_{1q}^T)_i^n (\partial G_{1q} / \partial \phi)_{i+1}^n \right] (\alpha-1) / \Delta x \\ - \left[(\partial F_{2q}^T / \partial \phi)_i^n (G_{2q})_{i+1}^n + (F_{2q}^T)_i^n (\partial G_{2q} / \partial \phi)_{i+1}^n \right] / (\Delta x)^2 \quad (23c)$$

$$(d_i^n)_q = \left[\mathcal{D}(\phi^n) + S^n \right] / \beta \quad (23d)$$

When applied at successive grid points, Eq. (22) generates a block-tridiagonal system of equations for ψ^* which, after appropriate treatment of boundary conditions, can be solved efficiently using standard block-elimination methods as discussed by Isaacson and Keller (Ref. 23, p. 58). The solution procedure for Eqs. (17b&c) is analogous to that just described for Eq. (17a). It is worth noting that the spatial difference parameter α can be varied with i or even term by term. For example, an "upwind difference" formula can be obtained if α is chosen as 1 or -1 depending on the sign of the elements of F_1 .

Fourth-Order Spatial Differences

Fourth-order spatial accuracy can be obtained by using the following standard five-point difference formulas in place of Eqs. (19):

$$D_{\tilde{x}}\phi = \frac{1}{2\Delta\tilde{x}} \left(1 - \frac{1}{6}\Delta_+\Delta_-\right) (\Delta_+\Delta_-\phi) = (\partial\phi/\partial\tilde{x})_i + o(\Delta\tilde{x}^4) \quad (24a)$$

$$D_{\tilde{x}}^2\phi = \frac{1}{(\Delta\tilde{x})^2} \left(1 - \frac{1}{12}\Delta_+\Delta_-\right) (\Delta_+\Delta_-\phi) = (\partial^2\phi/\partial\tilde{x}^2)_i + o(\Delta\tilde{x}^4) \quad (24b)$$

In this instance, the block-tridiagonal structure of Eq. (22) expands to block quindagonal. Block-quindagonal systems are easily solved using banded Gaussian block-elimination. The question arises, however, whether the increased accuracy thus obtained is worth the additional computation involved in solving block-quindagonal systems. This topic will be discussed subsequently.

Recently, there has been revived interest (Orszag & Israeli, Ref. 1) in the following fourth-order compact difference formulas involving only three grid points:

$$D_{\tilde{x}}\phi = \frac{1}{2\Delta\tilde{x}} \frac{(\Delta_+\Delta_+)}{(1 + \frac{1}{6}\Delta_+\Delta_+)} \phi = (\partial\phi/\partial\tilde{x})_i + o(\Delta\tilde{x}^4) \quad (25a)$$

$$D_{\tilde{x}}^2\phi = \frac{1}{(\Delta\tilde{x})^2} \frac{(\Delta_+\Delta_+)}{(1 + \frac{1}{12}\Delta_+\Delta_+)} \phi = (\partial^2\phi/\partial\tilde{x}^2)_i + o(\Delta\tilde{x}^4) \quad (25b)$$

To implement Eqs. (25) within the ADI framework, the difference equations are multiplied by the denominator of Eq. (25a) or (25b) at the appropriate step in the solution procedure (cf. Mitchell, Ref. 14; Beam & Warming, Ref. 13).

The attraction of Eqs. (25) over (24) is that Eqs. (25) lead to block-tridiagonal rather than block-quindagonal equations. One difficulty which arises with Eqs. (25), however, is that the denominators are different and must be removed separately when both first and second order derivatives are present, as in the Navier-Stokes equations. Consequently, first and second derivative terms require a separate step in the ADI procedure, and thus two block-tridiagonal systems must be solved for Eqs. (25), as opposed to one block-quindagonal system for Eqs. (24), in each coordinate direction that both first and second derivatives appear. In terms of computational effort, these requirements are approximately equal, as will be shown in the following section, and from this standpoint, there is little to choose between Eqs. (24) & (25). Both Eqs. (24) and (25) suffer from complications in applying boundary conditions, as is usually the case when a difference formula is of higher

order than the derivative approximated. One disadvantage of Eqs. (25) is that the evaluation of explicit derivatives requires the solution of a simple tridiagonal system for each dependent variable present. Another limitation of Eqs. (25) arises when terms containing derivatives with nonconstant coefficients are present, for example, variable viscosity terms. Each nonconstant coefficient can be removed by division prior to clearing the denominator of Eqs. (25), but as a consequence, each term of this type in the same governing equation also requires a separate step in the ADI procedure, and the solution of a block-tridiagonal system. The authors are thus inclined to favor the five-point formulas Eqs. (24), since their use and efficiency is less dependent on the form of the governing equations.

Computing Requirements

Various block-elimination algorithms can be devised for solution of equations with block-banded matrix structures (cf., Isaacson & Keller, Ref. 23). Such algorithms can be derived using variants of Gaussian elimination for a banded matrix, but with the square submatrix elements of the banded matrix processed using matrix algebra. Thus, operations involving matrix subelements are not assumed to commute, and division by a matrix subelement is accomplished by computing the inverse and multiplying. Following this procedure, the authors have developed algorithms for both block-tridiagonal and block-quindiagonal systems arising from the respective second and fourth-order difference formulas, Eqs. (19) & (24). Each algorithm requires only one inverse per grid point. A standard operation count (scalar multiplications and divisions) has been performed for systems with $L \times L$ block elements and N diagonal block elements, i.e., L coupled equations along N grid points. The block-tridiagonal scheme requires $(3N-2)(L^3 + L^2)$ operations, the same as the matrix factorization scheme of Isaacson and Keller (Ref. 23); the block-quindiagonal scheme requires $(7N-10)L^3 + (5N-6)L^2$ operations, which is only slightly more than twice the block-tridiagonal number.

Orszag and Israeli (Ref. 1, p. 284) have estimated that fourth-order schemes achieve results in the 5 percent accuracy range with approximately half the number of grid points in each direction, as compared with second-order schemes. Thus based on the foregoing estimate and operation counts, it is concluded that for one-dimensional problems, use of the fourth-order scheme is roughly equivalent in terms of accuracy and computational cost to using the second-order scheme with twice as many grid points. In two and three dimensions, however, the second-order scheme requires four and eight times as many grid points, respectively, to obtain accuracy comparable to fourth-order schemes, and the fourth-order scheme is well worth the factor of two in computational effort per grid point.

Assuming there are N grid points in each coordinate direction, the total number of operations for a single time step is obtained from the operation count for solution of one block-banded system by multiplying by $2N$ and $3N^2$ for two and three dimensions, respectively.

For the particular case of the Navier-Stokes equations (3) with p eliminated using Eq. (6), it is possible to reduce the computational effort substantially by taking advantage of the special nature of the coupling during each ADI sweep. In this case, it is only necessary to solve one block-banded system with $L = 3$, as well as two simple banded systems ($L = 1$). This can be seen by careful examination of Eqs. (3). During the first step of the ADI procedure, only derivatives with respect to x and t from Eqs. (3) appear in the implicit difference equations. In the continuity, x momentum, and energy equations, these implicitly treated terms contain ρ , u , and T , but not v and w ; therefore, the difference equations from these three equations can be solved for ρ^* , u^* , and T^* during the first ADI step by solving a block-banded system with $L = 3$. Having obtained values for ρ^* , u^* , and T^* in this manner, the difference equations for the y and z momentum equations can then be solved independently for v^* and w^* ; since the y and z momentum equations are uncoupled with respect to v^* and w^* during this ADI step, the latter computation only requires the solution of two simple banded systems ($L = 1$). A similar situation exists for the remaining two steps of the ADI procedure, except that during the second step (y derivatives treated implicitly), the difference equations from the continuity, y momentum, and energy equations are solved as coupled equations for ρ^{**} , v^{**} , and T^{**} , and during the third step (z derivatives treated implicitly), the difference equations from the continuity, z momentum, and energy equations are solved as coupled equations for ρ^{n+1} , w^{n+1} , and T^{n+1} .

For tridiagonal systems, the operation count is reduced from order $450 N$ for one $L = 5$ system to order $118 N$ for one $L = 3$ and two $L = 1$ systems. For quindagonal systems, these estimates are $1000 N$ and $258 N$, respectively. Consequently, the arrangement leading to three coupled and two uncoupled equations is quite worthwhile. For comparison, it is noted that in the case of the Navier-Stokes equations (3), merely evaluating the right-hand side of Eq. (17a), which would be a minimum requirement for a one-step explicit scheme, requires $302 N$ operations for a 3-point difference formula and $488 N$ operations for a 5-point formula.

In view of the many factors involved, it is difficult to evaluate precisely or with any generality the overall computational efficiency of the present method relative to various other methods. However, the foregoing operational counts show that the effort expended to solve the implicit difference equations by block-elimination is not excessive compared with that necessary simply to evaluate the differenced Navier-Stokes equations, let alone the various other bookkeeping tasks present in most large-scale computer programs for fluid dynamics problems. In the solutions presented here, the solution of the tridiagonal and block-tridiagonal systems using double precision arithmetic required only about one third to one half of the total computer time per time step.

APPLICATION TO FLOW IN A STRAIGHT DUCT

Problem Formulation and Boundary Conditions

To explore the stability properties and general capabilities of the present method, some test calculations were made for three-dimensional laminar subsonic flow in the entrance region of a straight duct with rectangular cross section. The straight duct geometry was chosen for its simplicity, and consideration was limited to subsonic flow to avoid the possible occurrence of shocks. A consideration of shocks and other complicating factors which would have hindered the orderly development of the method is reserved for future studies. Application of the present method is straightforward once H , S , and \mathcal{D} are identified, and for the present calculations, these quantities are given in the Appendix. In applying the numerical method, the dissipation term, Φ , defined by Eq. (5), and the viscous terms in Eq. (4) containing $\nabla \cdot U$ were treated explicitly by evaluation at the n level. This is accomplished by setting $\beta = 0$ in Eq. (14b). Although Φ could be treated implicitly and linearized, this would unnecessarily complicate the difference equations. The viscous terms involving $\nabla \cdot U$ contain mixed derivatives whose treatment by ADI methods is somewhat awkward, as mentioned previously. For the solutions presented here and other test cases computed while developing the method, the explicit treatment of the aforementioned viscous and dissipation terms had no observable adverse affect on stability. All solutions presented here were made using three-point centered difference formulas [i.e., $\alpha = 1/2$ in Eq. (19)], and since steady solutions were the primary objective, the backward time difference form ($\beta = 1$) was employed throughout. In each case, the reference length, L_r , was taken as the duct width, and values of 0.73 and 1.4 were used for Pr and γ , respectively.

The flow geometry and coordinate system are shown in Fig. 1. Boundary and initial conditions are required to complete the problem formulation. It is assumed that the duct is fed from a large stagnant reservoir and exhausts into a constant-pressure reservoir. As an approximation to these conditions, the isentropic stagnation temperature, T_0 , and stagnation pressure, P_0 , are specified as upstream boundary conditions, and the static pressure, P_s , is specified as a downstream condition. These quantities can be written in nondimensional form as

$$T_0 = T + \left(\frac{\gamma - 1}{2} \right) M^2 w^2 \quad (26a)$$

$$P_0 = \frac{1}{\gamma M^2} \rho T \left(\frac{T}{T_0} \right)^{\gamma / (1 - \gamma)} \quad (26b)$$

$$P_s = \frac{1}{\gamma M^2} \rho T \quad (26c)$$

The u and v velocity components are small and were neglected in the definition of T_o . Including the u and v components in the definition of T_o would couple all five governing equations at the upstream boundary during the z -direction step of the ADI procedure. Unless u and v were treated explicitly, this coupling would preclude, during this ADI step, the use of the more efficient solution technique previously described, in which only three equations are coupled. Implicit boundary conditions are obtained by writing Eq. (26) at the $(n + 1)$ level and linearizing by the same procedure employed for the governing equations at interior points. The specified downstream static pressure, P_g , was an estimate of that required to maintain an average nondimensional velocity of 1.0 at the duct entrance. Additional boundary conditions are required at the upstream and downstream boundaries. The relation $D_z^2 w^{n+1} = 0$ was used at points adjacent to the upstream boundary. This boundary condition is equivalent to a linear extrapolation of w^{n+1} on the upstream boundary from values at the two adjacent interior points (on a line in the z direction), and will be referred to subsequently as implicit linear extrapolation.

As the remaining upstream boundary conditions, the normal derivatives of u^{n+1} and v^{n+1} are set equal to zero using three-point, second-order, one-sided difference approximations. At the downstream boundary, implicit linear extrapolation relations were used for T^{n+1} , u^{n+1} , v^{n+1} , and w^{n+1} , together with the static pressure relation. No-slip conditions were specified on the walls of the duct, and adiabatic conditions were imposed by setting normal derivatives of temperature to zero using three-point, one-sided difference formulas. In addition, the wall density was determined implicitly using a three-point, one-sided difference approximation of the continuity equation. Since the flow is symmetric about the horizontal and vertical planes passing through the duct centerline, solutions were computed for one quadrant of the duct, and symmetry conditions were imposed on these planes of symmetry.

Stability Tests

Computed Solutions

Two sequences of solutions were computed for $Re = 60$ with a $6 \times 6 \times 6$ grid and using different time steps, to explore the stability properties of the method. To provide a frame of reference, stability numbers N_{CFL} and N_{Re} are defined as the ratio of the actual time step Δt to the maximum allowable time step as determined by the CFL and viscous stability limits, respectively, for one dimensional uniform flow at the reference velocity and Mach number. These stability numbers are given by

$$N_{CFL} = \frac{\Delta t}{\Delta z} \left(1 + \frac{1}{M} \right) \quad (27a)$$

$$N_{\mu} = \frac{2}{\text{Re}} \frac{\Delta t}{(\Delta z)^2} \quad (27b)$$

Typically, conditionally stable methods would require $N_{\text{CFL}}, N_{\mu} \leq 1$ for stability. Multidimensional forms of Eq. (27) are more restrictive; however, splitting techniques can be employed (cf. MacCormack & Paullay, Ref. 24) to recover the one-dimensional forms. In actual computations with a conditionally stable method, the stability limits would vary from point to point with the local velocity, Mach number, and mesh size; however, Eq. (27) provides convenient reference quantities.

The initial conditions used for the stability tests are those appropriate for uniform flow in the z direction at the reference velocity and with the specified stagnation pressure and temperature. At $t = 0$, the no-slip conditions were applied and the downstream static pressure was impulsively reduced to P_s . The duct geometry has $x_1 = y_1 = 1$, $z_1 = 0.5$.

The downstream centerline value of $(w^{n+1} - w^n)/\Delta t$ is a sensitive indicator of steady-state conditions and is shown in Fig. 2 for a sequence of solutions with $M = 0.44$. It can be seen that the method gave stable solutions for test cases in the range $N_{\text{CFL}} \leq 43.2$, $N_{\mu} \leq 4.4$, and that steady conditions were reached with significantly fewer time steps for higher N_{CFL} . A second sequence of solutions was computed for $M = 0.044$, and similar results were obtained (Fig. 3) for $N_{\text{CFL}} \leq 1471$, $N_{\mu} \leq 20.6$.

The transient accuracy of the $M = 0.44$ test cases can be assessed in Fig. 4, although as mentioned earlier, transient accuracy was not an objective of these calculations. The solutions in Fig. 4 are not independent of the time step (N_{CFL}), and thus there is temporal truncation error in these solutions. However, curves a & b display far less dependence on N_{CFL} than the remaining curves, and thus it appears that convergence is beginning for $N_{\text{CFL}} \leq 2.2$. Steady-state conditions are reached in a nondimensional time on the order of 4 for curves a & b. Clearly, the temporal truncation error is much greater for curves c & d ($10.8 \leq N_{\text{CFL}} \leq 21.6$), although these latter cases reached steady state in fewer time steps (Fig. 2). Similar plots of the transient solution for the $M=0.044$ test cases are given in Fig. 5.

It should be emphasized that the degree of transient accuracy indicated in Figs. 4 and 5 is not a general indication of the accuracy achievable at a given N_{CFL} or N_{μ} with the present method, since these stability tests involve first-order backward time differences, a very coarse mesh, and impulsive starting conditions.

Solutions attempted for $N_{CFL} = 108$ ($M=0.44$) and $N_{CFL} = 14,710$ ($M = 0.044$) were unstable. Although the precise cause of the instability is unknown, the difficulties did appear to originate near the boundaries. Since solutions to Eq. (17) in general need exist only for sufficiently small Δt , one possible explanation other than the obvious one of a conventional instability is that the system of implicit difference equations is near singular for these step sizes.

Although possibly by coincidence, it is noted that the breakdown occurred for time steps which were larger than the apparent time periods ($t \approx 4$) of the physical transients as determined in Figs. 4 and 5.

The effect of mesh size on computed solutions was examined empirically for the $M=0.44$ test case. Axial velocity profiles are compared in Fig. 6 for two solutions having $6 \times 6 \times 6$ and $11 \times 11 \times 11$ grids in the computed quadrant of the duct; the two solutions are in satisfactory agreement. The error is larger at the duct entrance, where the inlet conditions are somewhat severe for the mesh spacing used. In Fig. 7, centerline velocity and pressure are shown for three solutions having 6, 11, and 21 mesh points in the z direction. This comparison also reflects a reasonable influence of mesh size on the solutions.

Solution With Moving Wall

An additional solution was computed for $M=0.44$, $Re = 60$ but with a large secondary flow caused by moving two parallel duct walls in a direction perpendicular to the axial flow direction; the wall speed is about 25 percent of the average axial velocity. Since the flow is symmetric about a horizontal plane midway between the moving walls, only the lower half of the flow field was computed, and computer-produced drawings of selected streamlines for this solution are shown in Fig. 8. No data or other theoretical studies are available for comparison in this instance and the computed solutions are presented largely as a demonstration of stability in the presence of large secondary flows.

High Reynolds Number Solutions

Nonuniform-Grid Transformation

The accuracy of solutions computed with a given number of grid points can often be improved by using a nonuniform grid spacing to ensure that grid points are closely spaced in regions where the solution varies rapidly and widely spaced elsewhere.

An analytical coordinate transformation has been devised by Roberts (Ref. 25) which is an effective means of introducing a nonuniform grid when the steep

gradients occur near the computational boundaries. If N grid points are to be used in the range $0 \leq x \leq 1$, and if steep gradients are anticipated in a region of thickness σ near $x = 0$, then Roberts' transformation $\eta(x)$ is given by

$$\eta(x) = N + (N-1) \log \left(\frac{x+a-1}{x+a+1} \right) / \log \left(\frac{a+1}{a-1} \right) \quad (28)$$

where $a^2 = 1/(1 - \sigma)$. The use of equally-spaced points in the transformed coordinate η provides resolution of both the overall region $0 \leq x \leq 1$ and the subregion $0 \leq x \leq \sigma$. The transformation (28) was employed in high Reynolds number solutions to provide increased resolution near the duct entrance and in boundary layers on the duct walls. Values of 0.1, 0.1, and 0.25 were used as σ for the x , y , and z coordinates, respectively.

Artificial Dissipation

In computing solutions for high Re , it was necessary to add a form of artificial viscosity or dissipation for the axial flow direction. Artificial dissipation in some form is often useful in practical calculations to stabilize the overall method when boundary conditions are treated inaccurately, when coarse mesh spacing is used, or in the presence of discontinuities. [Von Mises (Ref. 26) has shown that certain discontinuities in solutions of the Navier-Stokes equations are possible despite the presence of physical viscosity and heat conduction terms.] The need for artificial dissipation arises in certain instances when centered spatial difference approximations are used for first derivative terms. The use of artificial dissipation is thus a matter of spatial differencing technique, and is commonly employed in either explicit or inherent form and in both explicit and implicit difference schemes. The particular form described here was adequate for present purposes but is considered provisional and is not recommended for general use, since the formal accuracy is lowered to first order for the axial (z) coordinate direction.

The dissipation term used here is based on an observation (e.g., Roache, Ref. 27, p. 162) that for a linear model problem representing a one-dimensional balance of convection and diffusion terms, solutions obtained using central differences for the convection term are well behaved provided the mesh Reynolds number $Re_{\Delta z} = |w| \Delta z / \nu$ is ≤ 2 , but that qualitative inaccuracies (associated with boundary conditions) occur for $Re_{\Delta z} > 2$. This suggests the use of an artificial viscosity term of the form $\epsilon_z D_z^2 \phi$, where

$$\epsilon_z = \begin{cases} \frac{|w| \Delta z}{2} - \frac{\nu}{Re} = \frac{\nu}{Re} \left(\frac{Re_{\Delta z}}{2} - 1 \right) & Re_{\Delta z} > 2 \\ 0 & Re_{\Delta z} \leq 2 \end{cases} \quad (29)$$

to ensure that the local effective mesh Reynolds number is no greater than two. This dissipation term was added to each of the governing equations, with ϕ taken as ρ for the continuity equation, u , v , w for the respective x , y , and z momentum equations, and T for the energy equation. For scalar equations, the foregoing technique is equivalent to that developed by Spalding (Ref. 28) from an argument not involving artificial viscosity.

Computed Solution

A solution is presented for $M=0.3$, $Re = 600$ and a duct geometry for which $x_1 = y_1 = 1$, $z_1 = 5$. An $11 \times 11 \times 21$ grid was used, along with a variable time step with N_{CFL} up to 380 and, N_{μ} up to 12.

Computed axial velocity profiles at the duct entrance and exit are shown in Fig. 9 for this case. The subscript 1 denotes conditions at the duct entrance. The axial variation of pressure ratio and Mach number is given in Fig. 10. As a check on the solution, two additional pressure curves are shown. One curve represents the pressure ratio from one-dimensional theory for adiabatic, frictional, constant-area flow of a perfect gas (Shapiro, Ref. 29). Using this theory, the pressure ratio between two points can be evaluated if the Mach numbers are known; the average Mach number, M_{avg} , (averaged over the cross section) from the Navier-Stokes solution was used for this evaluation. The second curve assumes isentropic flow and constant stagnation pressure along the centerline of the duct and was evaluated from the isentropic relations for a perfect gas using the computed centerline Mach number, M_D . The general agreement of pressure ratio distributions seen in Fig. 10 is an indication of internal consistency in the computed solution. Since the average inlet Mach number is only 0.27, and since the axial variation in density is only about 8 percent, compressibility effects should be relatively minor for this solution. The computed pressure drop was therefore compared with the experimental measurements of Beavers, Sparrow, and Magnuson (Ref. 30) for incompressible flow and found to be in reasonable agreement, considering the difference in M . The results of this comparison are shown in Fig. 11.

In assessing the high Reynolds number solution, the question arises as to whether the artificial viscosity destroys the accuracy by changing the effective Reynolds number of a viscous calculation. Here, it should be emphasized that the artificial viscosity was used only for the axial coordinate direction, where viscous terms are generally unimportant; second-order accuracy was rigorously maintained for the two transverse directions, for which viscous stresses are large. The magnitude of the artificial viscosity terms in the computed solutions was examined a posteriori and compared with other terms in the equations. It was found that the artificial viscosity terms were no greater than about 2 percent of the largest term in each equation, except at grid points very near the edges

of the duct walls at the entrance. The specification of constant stagnation pressure and temperature at the entrance along with the no-slip conditions on the walls produces very large gradients in this region, and the artificial viscosity terms were as large as 15 to 20 percent there. It is believed, however, that the accuracy was not seriously degraded by the artificial viscosity except, of course, locally near the entrance edges of the walls. As a final check on the solutions, the mass flow rate was computed by integration of w over the cross section at each axial location in the duct and was found to be constant to within 0.4 percent.

The UNIVAC 1108 run time for the solutions presented here was about 3.5×10^{-4} minutes per grid point per time step, which includes the use of auxiliary storage devices. Solution of the implicit difference equations was performed in double precision. Convergence to a steady solution required from 20 to 100 time steps, depending on how the time step was chosen.

Convergence Acceleration Tests

In the solutions presented to this point, a constant or more or less monotonically increasing time step was used, and this time step was selected on the basis of rough estimates of the physical time scales present in the transient evolution toward steady state. However, when transient accuracy is of no concern (as is the case for computing steady solutions), the time step can be regarded as an iteration parameter which can be selected so as to speed up the convergence to a steady solution. In previous studies in which ADI methods have been used to solve iteratively scalar elliptic equations such as Poisson's equation, it has been established (Ref. 31) that a significant improvement in rate of convergence can be achieved by the cyclic use of a sequence of acceleration parameters (time steps) of differing magnitude, rather than a single parameter. This concept was explored to a limited extent for application to the Navier-Stokes system of equations. A sequence of solutions to a sample problem was computed in which single (constant) time steps of various sizes were used. The sample problem consisted of two-dimensional laminar flow in a straight channel with a length to width ratio of 10:1, with $M = 0.5$ and $Re = 300$, and using an 11×11 grid. By comparing the transient solutions and convergence rates for the different time steps, it was established that the optimum single time step for this problem was about 0.1 times the time required for a particle to pass through the channel at the average flow velocity, and that about 25 time steps were required to reach steady state in this instance. A sequence of time steps was then selected and used cyclically to determine whether any increase in convergence rate could be achieved. For the particular test case and time step sequence considered, there was only a minor improvement over the convergence rate for the optimum single time step. However, as shown in Ref. 31 for Laplace's equation,

the improvement in convergence rate brought about by parameter sequences is greatly enhanced when the spatial mesh is refined. Since the present tests were run with a very coarse mesh (to minimize computing costs), the tests are inconclusive with regard to the convergence rate of fine mesh calculations, which are of considerable practical importance. Finally, it is noted that the optimum time step corresponded to N_{CFL} of about 100.

APPLICATION TO TURBULENT FLOW IN A STRAIGHT DUCT

Background

Since many practical flows at high Reynolds number are turbulent, it is desirable to have the capability to treat various turbulence models within the present numerical framework. Consequently, some test calculations were made for turbulent flow in the same rectangular duct geometry used in the previous laminar calculations, as a means for exploring the applicability of the present method to the computation of turbulent flows. The straight duct geometry is convenient for such an exploratory study, not only because of its relative simplicity, but also because there are some previous experimental and numerical results (e.g., Ahmed & Brundrett, Ref. 32; Launder & Ying, Ref. 33) available for comparison. For the present calculations, a relatively simple turbulence model, consisting of an eddy viscosity formulation and specified mixing length is employed. The shortcomings of this approach (e.g., the difficulty is selecting a suitable mixing length distribution in advance) are well known, and a number of more advanced turbulence models are currently being developed (cf. Launder & Spalding, Ref. 34) wherein various turbulence quantities are determined as the (numerical) solution of one or more "turbulence equations". A number of these more advanced turbulence models employ a turbulent viscosity as a means of relating the turbulent stresses to the mean flow, however, and the present computational problem is therefore similar in many respects to that which would occur with one of the more advanced turbulence models. Thus, alternative and less restrictive turbulence models can be incorporated into the present computational framework in a future study.

Turbulence Model

To account for turbulent transport processes, the governing equations are time-averaged in the usual manner for turbulent flows (e.g., Hinze, Ref. 35). The dependent variables are represented as the sum of a time-averaged quantity denoted by an overbar ($\bar{}$) and an instantaneous fluctuating quantity denoted by a prime (\prime). This process of averaging produces turbulent correlations which are conventionally termed Reynolds stresses.

The time averaging is performed over a period of time sufficiently long to remove the random turbulent fluctuations, but not so long as to remove the time dependence of the mean flow. Since the present calculations are limited to subsonic flow, it is reasonable to neglect turbulent fluctuations in density. In addition, the assumption that the total enthalpy is a constant E_0 was made, and thus, pressure is eliminated from the momentum equations by means of Eq. (8). As indicated previously, it is no longer necessary to solve the energy equation. After time averaging, the Navier-Stokes equations can be written in a form identical to Eqs. (3a-b), except that the force due to viscous stress F now includes both laminar and turbulent stresses.

In discussing the turbulence model, Cartesian tensor notation is employed, and thus, the subscripts i and j , previously used to denote a discretized variable, will be used to denote the components of velocity $u_i = u, v, w$, and the space coordinates $x_i = x, y, z$. The components F_i of the force due to viscous stress can thus be written as

$$F_i = \frac{\partial}{\partial x_j} (2\overline{\mu e_{ij}}) - \frac{\partial}{\partial x_j} (\rho \overline{u_i u_j}) \quad (30)$$

where the rate of strain tensor e_{ij} is given by

$$e_{ij} = \frac{1}{2} (\partial u_i / \partial x_j + \partial u_j / \partial x_i) \quad (31)$$

The Reynolds stress terms $\rho \overline{u_i u_j}$ are related to the mean flow variables by means of the Boussinesq eddy viscosity concept (cf. Hinze, Ref. 35), from which

$$\rho \overline{u_i u_j} = -2\mu_T \overline{e_{ij}} + \frac{1}{3} \rho \overline{u_k u_k} \delta_{ij} \quad (32)$$

where μ_T is the eddy or turbulent viscosity and $\overline{e_{ij}}$ is the mean flow rate of strain tensor. With the further assumption that laminar viscosity fluctuations are negligible, Eq. (30) becomes

$$F_i = 2 \frac{\partial}{\partial x_j} [(\mu + \mu_T) \overline{e_{ij}}] - \frac{1}{3} \frac{\partial}{\partial x_i} (\rho \overline{u_k u_k}) \quad (33)$$

It remains to relate the eddy viscosity μ_T to the mean flow variables. This is accomplished by means of a mixing length hypothesis of the form

$$\mu_T = \rho l^2 (2 \underline{\underline{e}} : \underline{\underline{e}})^{1/2} \quad (34)$$

One possibility for specifying the mixing length l is provided by the following empirical one-parameter family developed by McDonald and Camarata (Ref. 35) on the basis of experimental evidence for two-dimensional turbulent boundary layers:

$$\frac{l}{\delta_b} = \frac{l_\infty}{\delta_b} \tanh\left(\frac{\kappa \hat{y}}{l_\infty}\right) \mathcal{D}_s \quad (35)$$

where δ_b is the local boundary layer thickness, κ is the von Karman constant, \hat{y} is the distance from the wall, and \mathcal{D}_s is a sublayer damping factor defined by

$$\mathcal{D}_s = \left[P \left(\frac{y^+ - \bar{y}^+}{\sigma^+} \right) \right]^{1/2} \quad (36)$$

where P is the normal probability function, and

$$y^+ = \hat{y} \left(\frac{\tau}{\rho} \right)^{1/2} \frac{\rho}{\mu} \quad (37)$$

Here τ is the local shear stress, $\bar{y}^+ = 23$ and $\sigma^+ = 8$.

Although the mixing length profile (35) of McDonald and Camarata (Ref. 35) was developed for two-dimensional boundary layers, it can be adapted for use in a rectangular duct by assuming, for example, that \hat{y} is the distance to the nearest wall. In a fully developed duct flow δ_b may be taken as the duct half-width, while in the developing region an approximate average value of δ_b could be calculated from the solution as it evolves in time. It remains to specify the parameter (l_{∞}/δ_b). For two-dimensional equilibrium turbulent boundary layers, l_{∞}/δ_b has a value near 0.09 (McDonald & Camarata, Ref. 35); for fully developed pipe and channel flows l_{∞}/δ_b is known to be approximately 0.14 (cf. Schlichting, Ref. 37). The use of $l_{\infty}/\delta_b = 0.14$ in Eq. (35) provides a close approximation to the mixing length distribution for a pipe as given by Schlichting (Ref. 37). Within the framework of the proposed mixing length model, Eq. (36), an empirical formula is required for the variation of l_{∞}/δ_b from 0.09 in the boundary layer region near the duct inlet to 0.14 in the fully developed region of the duct flow.

Sufficient information has been given to apply the foregoing turbulence model to flow in a square duct. One physical shortcoming of the model, however, is that it is based upon an isotropic turbulent viscosity, and it is known (cf. Launder & Ying, Ref. 33) that models of this type do not predict the experimentally observed secondary flows generated by the turbulence. The problem of steady fully-developed turbulent flow in a duct of square cross section was considered by Launder and Ying (Ref. 33), who modeled the Reynolds stress terms which induce the secondary motion. Brundrett and Baines (Ref. 38) also showed that transverse gradients in the Reynolds stresses result in the observed secondary-flow velocities in the cross-sectional plane.

Launder and Ying (Ref. 33) modeled the Reynolds stress terms ($\overline{u'^2} - \overline{v'^2}$) and $u'v'$ which appear in the vorticity equation. Here, the Launder - Ying approach is adapted for use with the present velocity-pressure formulation of the Navier-Stokes equations and this requires specification of the stresses $\overline{u'^2}$, $\overline{v'^2}$ and $u'v'$. To simplify the analysis, it was assumed that the approximations employed by Launder and Ying in modeling the Reynolds stresses for fully-developed flow are also sufficiently accurate in the developing region of a duct flow. The high Reynolds number analysis of Launder and Ying was based on the Reynolds stress transport equations, and neglected the convection and diffusion terms, and the generation terms in the equations for $\overline{u'^2}$, $\overline{v'^2}$ and $u'v'$. In addition, since the dissipation of turbulence energy at high Reynolds numbers is isotropic, the approximation

$$2\nu \frac{\partial u'_i}{\partial x_k} \frac{\partial u'_j}{\partial x_k} = \frac{2}{3} \delta_{ij} \epsilon \quad (38)$$

was introduced, where ϵ is the turbulence energy dissipation rate. With the above approximations the transport equations for $\overline{u'^2}$, $\overline{v'^2}$ and $\overline{u'v'}$ reduce to

$$\frac{\overline{p' \frac{\partial u'}{\partial x_1}}}{\rho} = \frac{1}{3} \epsilon + \overline{u'w'} \frac{\partial \overline{u}}{\partial x_3} \quad (39a)$$

$$\frac{\overline{p' \frac{\partial v'}{\partial x_2}}}{\rho} = \frac{1}{3} \epsilon + \overline{vw'} \frac{\partial \overline{v}}{\partial x_3} \quad (39b)$$

and

$$\frac{\overline{p' \left(\frac{\partial u'}{\partial x_2} + \frac{\partial v'}{\partial x_1} \right)}}{\rho} = 0 \quad (39c)$$

Following Launder and Ying, the approximations for the correlations between pressure and velocity-gradient fluctuations are modeled using the form suggested by Hanjalic and Launder (Ref. 39), which was based on earlier work by Rotta (Ref. 40). There results

$$\frac{\overline{p' \frac{\partial u'}{\partial x_1}}}{\rho} = \frac{c_1}{3} \epsilon - \frac{\overline{u'^2}}{2k} (c_1 \epsilon - 2c_2 P_k) + \beta (2\overline{u'w'} \frac{\partial \overline{w}}{\partial x_1} + \overline{v'w'} \frac{\partial \overline{w}}{\partial x_2}) \quad (40a)$$

$$\frac{\overline{p' \frac{\partial v'}{\partial x_2}}}{\rho} = \frac{c_1}{3} \epsilon - \frac{\overline{v'^2}}{2k} (c_1 \epsilon - 2c_2 P_k) + \beta (\overline{u'w'} \frac{\partial \overline{w}}{\partial x_1} + \overline{v'w'} \frac{\partial \overline{w}}{\partial x_2}) \quad (40b)$$

and

$$\frac{\overline{p' \left(\frac{\partial u'}{\partial x_2} + \frac{\partial v'}{\partial x_1} \right)}}{\rho} = -\frac{\overline{u'v'}}{k} (c_1 \epsilon - 2c_2 P_k) + \beta (\overline{v'w'} \frac{\partial \overline{w}}{\partial x_1} + \overline{u'w'} \frac{\partial \overline{w}}{\partial x_2}) \quad (40c)$$

where k is the turbulence kinetic energy, P_k is the rate of production of turbulence kinetic energy, c_1 and c_2 are constants, and $\beta = (6c_2 - 2)/11$. The production term P_k is given by (Ref. 33),

$$P_k = -\overline{u'w'} \frac{\partial \overline{w}}{\partial x_1} - \overline{v'w'} \frac{\partial \overline{w}}{\partial x_2} \quad (41)$$

and for nearly equilibrium turbulence, one may assume that ϵ is equal to P_k .

The use of Eqs. (39-41) results in the following expressions for $\overline{u'^2}$, $\overline{v'^2}$ and $\overline{u'v'}$:

$$\overline{u'^2} = c_3 \frac{k}{\epsilon} \overline{u'w'} \frac{\partial \overline{w}}{\partial x_1} - c_4 \frac{k}{\epsilon} P_k \quad (42a)$$

$$\overline{v'^2} = c_3 \frac{k}{\epsilon} \overline{v'w'} \frac{\partial \overline{w}}{\partial x_2} - c_4 \frac{k}{\epsilon} P_k \quad (42b)$$

$$\overline{u'v'} = \frac{c_3}{2} \frac{k}{\epsilon} (\overline{v'w'} \frac{\partial \overline{w}}{\partial x_1} + \overline{u'w'} \frac{\partial \overline{w}}{\partial x_2}) \quad (42c)$$

where the constants are

$$c_3 = \frac{2(6c_2 - 2)}{11(c_1 - 2c_2)} \quad (43a)$$

$$c_4 = \frac{2}{c_1 - 2c_2} \left(\frac{c_1 - 1}{3} - \frac{6c_2 - 2}{11} \right) \quad (43b)$$

The remaining Reynolds stress terms $\overline{u'w'}$ and $\overline{v'w'}$ are modeled using Eq. (32), i.e.,

$$\overline{u'w'} = -\nu_T \frac{\partial \overline{w}}{\partial x_1}; \quad \overline{v'w'} = -\nu_T \frac{\partial \overline{w}}{\partial x_2} \quad (44)$$

The effective turbulence kinematic viscosity $\nu_T = \mu_T/\rho$ for the Reynolds stress model is obtained from the Prandtl-Kolmogorov formula:

$$\nu_T = c_\nu k^{1/2} \ell_w \quad (45)$$

and following Launder and Ying, ϵ is approximated by

$$\epsilon = c_D k^{3/2} / \ell_w \quad (46)$$

where ℓ_w is a turbulence length scale. Furthermore, from Eq. (41),

$$P_k = \nu_T \left[\left(\frac{\partial \overline{w}}{\partial x_1} \right)^2 + \left(\frac{\partial \overline{w}}{\partial x_2} \right)^2 \right] \quad (47)$$

and thus, Eqs. (42) reduce to

$$\overline{u'^2} = -c \ell_w^2 \left(\frac{\partial \overline{w}}{\partial x_1} \right)^2 + c_5 \ell_w^2 \left[\left(\frac{\partial \overline{w}}{\partial x_1} \right)^2 + \left(\frac{\partial \overline{w}}{\partial x_2} \right)^2 \right] \quad (48a)$$

$$\overline{v'^2} = -c_l \ell_w^2 \left(\frac{\partial \overline{w}}{\partial x_2} \right)^2 + c_5 \ell_w^2 \left[\left(\frac{\partial \overline{w}}{\partial x_1} \right)^2 + \left(\frac{\partial \overline{w}}{\partial x_2} \right)^2 \right] \quad (48b)$$

$$\overline{u'v'} = -c_l \ell_w^2 \left(\frac{\partial \overline{w}}{\partial x_1} \right) \left(\frac{\partial \overline{w}}{\partial x_2} \right) \quad c = c_3 c_\nu / c_D, \text{ and } c_5 = c_4 c_\nu / c_D \quad (48c)$$

where $c = c_3 c_\nu / c_D$, and $c_5 = c_4 c_\nu / c_D$.

The length scale ℓ_w must be specified in the above model. Launder and Ying (Ref. 33) used the form suggested by Buleev (Ref. 41).

$$\frac{1}{\ell_w} = \frac{1}{2} \int_0^{\partial \pi} \frac{d\phi}{s} \quad (49)$$

where the notation is explained in Fig. 12.

An interesting observation can be made about the Launder-Ying turbulence model for the case of equilibrium turbulence, i.e., $\epsilon = P_k$. It is easily seen that Eqs. (45-47) reduce to the form of Eq. (34), i.e.,

$$\nu_T = \ell_m^2 \left[\left(\frac{\partial w}{\partial x_1} \right)^2 + \left(\frac{\partial w}{\partial x_2} \right)^2 \right]^{1/2} \quad (50)$$

with the implied mixing length, ℓ_m , given by

$$\ell_m = \kappa \ell_w \quad (51)$$

As stated by Launder and Ying (Ref. 33), the Buleev length scale ℓ_w , Eq. (49), provides a nonrigorous but plausible method of accounting for the influence of adjacent walls in the duct. On further examination, the Buleev length scale is found to have the property that the mixing length distribution from Eq. (51) along a plane of symmetry is nearly the same as that for a fully developed pipe flow (cf, Ref. 37), and significantly, it yields $\ell_m \rightarrow \kappa y$ near the wall and a value of 0.14 at the center of the duct.

The present adaptation of the Launder-Ying model, Eqs. (48-49), provides the correlations between transverse velocity component fluctuations required in the transverse momentum equation force terms, Eq. (30). In the x_1 - momentum equation,

$$F_1 = -\frac{\partial}{\partial x_1} (\rho \overline{u'^2}) - \frac{\partial}{\partial x_2} (\rho \overline{u'v'}) - \frac{\partial}{\partial x_3} (\rho \overline{u'w'}) + \frac{\partial}{\partial x_j} (\partial \mu \overline{e_{ij}}) \quad (52a)$$

and in the x_2 momentum equation

$$F_2 = -\frac{\partial}{\partial x_1}(\rho \overline{u'v'}) - \frac{\partial}{\partial x_2}(\rho \overline{v'^2}) - \frac{\partial}{\partial x_3}(\rho \overline{v'w'}) + \frac{\partial}{\partial x_j}(2\mu \overline{e}_{2j}) \quad (52b)$$

In these expressions the first two terms are obtained from Eqs. (48) and the third term is obtained from Eq. (44), with the turbulent viscosity μ_T specified by Eq. (34).

Special consideration must be given to calculation of turbulent flow in the vicinity of walls in view of the large flow gradients which occur there. Since the expense of simply increasing the number of grid points near a wall may be considerable, an analytical wall function formulation has been employed in the present study. A set of three universal velocity profiles (cf, Walz, Ref. 42) is employed in the wall region, corresponding to the laminar sublayer ($y^+ \leq 4$), a transition region ($4 < y^+ < 26$), and the logarithmic law-of-the-wall region ($y^+ \geq 26$):

$$u^+ = y^+ \quad \text{for } y^+ \leq 4 \quad (53a)$$

$$u^+ = c_1 \ln(1+y^+) + c_2 + [(1-c_1-c_2 a)y^+ - c_2] e^{-ay^+} \quad \text{for } 4 < y^+ < 26 \quad (53b)$$

$$u^+ = c_1 \ln y^+ + c_2 \quad \text{for } y^+ \geq 26 \quad (53c)$$

where

$$u^+ = \hat{u}/u^* \quad (54)$$

$$y^+ = \hat{y}(\rho u^* Re) \quad (55)$$

and

$$u^* = (\tau_w/\rho)^{1/2} \quad (56)$$

In Eq. (54) \hat{u} denotes the total velocity component parallel to the wall, u^* is the nondimensional friction velocity, Eq. (56), and τ_w is the wall shear stress. The constants c_1 , c_2 , and a in Eqs. (53) were taken as 2.5, 5.1, and 0.3, respectively. The finite difference form of the velocity gradient at the grid point adjacent to the wall point is specified consistent with the appropriate universal profile given above. In the present formulation the assumption of constant shear stress in the immediate vicinity of the wall is utilized. The specification of the velocity gradient at the grid point adjacent to the wall (where the velocity is known) is equivalent to imposing a "slip" velocity at the wall itself. Hence, flow resolution in the region very near the wall is sacrificed to attain accuracy in the central region of the flow field. However, if accurate calculations in the wall region are required at a later date, refinements to the wall function approach may be implemented easily in the present computational procedure.

In the incorporation of the turbulence model into the numerical solution procedure, it is, of course, recognized that the turbulent viscosity μ_T ultimately depends on the mean flow variables. It is impractical to attempt to linearize μ_T rigorously, however, as the partial derivatives of μ_T with respect to the mean flow variables are not easily obtained. Consequently, for the present calculations, μ_T was evaluated at the n time level after each time step and lagged during the implicit computation procedure, i.e., μ_T was treated numerically as a given function of the space coordinates.

Computed Solutions

The flow conditions present in the measurements of Ahmed and Brundrett (Ref. 32) of the mean flow properties in the developing region of a square duct were adopted as a suitable test case. The experimental configuration (Ref. 32) consisted of a 3.625 in. square duct with a length of 18 feet. Ahmed and Brundrett presented isovels (axial velocity contours in the cross-sectional plane) at a Reynolds number, $Re_M = \rho_r U_r D_M / \mu_r$ based on the modified length scale $D_M = \sqrt{2} D_H$ (where $D_H = 3.625$ in.), of approximately 1.065×10^5 . Experimental static pressure distributions (Fig. 3a of Ref. 32) in the axial direction were given at Reynolds numbers, Re_M , of 0.59×10^5 , 1.076×10^5 , 1.41×10^5 , and 1.58×10^5 for a duct with a gradual entrance. The static pressure distribution for $Re_M = 1.076 \times 10^5$ from Ref. 32 provides the pressure drop required in the calculation procedure for a specified section of the duct length.

As a preliminary step prior to consideration of the developing flow, the fully developed flow near the end of the duct was computed to assess the various components of the foregoing turbulence model. The eddy viscosity turbulence model, Eqs. (33-34), along with the mixing length from either Eq. (35) or (51), was first employed without the Launder-Ying modifications (Eq. 42) to obtain predictions without a turbulence-driven secondary flow. Unfortunately, at the time of the present writing, a satisfactory solution could not be obtained with the modified Launder-Ying secondary flow model employed in the present numerical procedure, and thus none of the solutions presented contain a turbulence-driven secondary flow. The cause of the difficulty with the secondary flow turbulence model is presently under investigation and is possibly in the treatment of boundary conditions or the assumption of a quasisteady turbulence model, which results in an absence of time derivatives in the turbulence model.

For the fully developed flow region, a duct section of length $5D_H$ was chosen and the pressure drop was taken as 10.21 Pa (1.042 mm H_2O). The boundary conditions appropriate for fully developed flow are a specified constant static pressure at the upstream and downstream boundaries. The static pressure condition is satisfied by linearizing Eq. (8) about t^n using the same procedure that was employed for the governing equations. In place of the no-slip conditions on the duct walls, the wall function analysis discussed previously was used for velocity components parallel to the wall. Otherwise, the boundary conditions were identical to those employed in the laminar calculations. Symmetry conditions were employed at the planes of symmetry, passing through the duct centerline, and the solution was computed for one quadrant of the duct.

Solutions were computed for a duct of length $5D_H$ using a $10 \times 10 \times 6$ grid with the Roberts transformation (Ref. 28) applied in the transverse coordinate directions to improve accuracy near the walls. It should be noted that reducing the Roberts parameter σ from 0.5 to 0.1 had a negligible effect on the computed mass

flow rate and overall skin friction. Also, integral momentum conservation checks performed using the calculated wall shear stress and axial pressure gradient showed that the calculated axial momentum flux was conserved to within 2.5 percent.

Axial velocity contours calculated with the mixing length Eq. (51) are shown in Fig. 13 along with the measurements of Ahmed and Brundrett (Ref. 32) which were taken at the location $Z/D_H = 26.2$ at a Reynolds number $Re_H = 0.881 \times 10^5$. The comparison clearly shows the distortion of the measured isovels due to convection of high momentum fluid from the duct center toward the corners, which is presumably due to the existence of secondary flows in the duct (Launder & Ying, Ref. 32) not modeled in the calculations. A comparison of calculated and measured values of skin friction coefficient shows some interesting features. The Preston tube measurements of Ahmed and Brundrett (Ref. 32) and the skin friction coefficient deduced from the measured pressure gradient in the fully developed region are shown in Fig. 14, along with the calculations of Launder and Ying (Ref. 33). Here, the skin friction coefficient is defined as $c_f = \bar{\tau}_w / (\frac{1}{2}\rho_r U_r^2)$, where $\bar{\tau}_w$ is the average wall shear stress, and the Reynolds number is given by $Re_H = \rho_r U_r D_H / \mu$. The present results shown in Fig. 14 were obtained using the mixing length models described by Eqs. (35) and (51) at two different Reynolds numbers (corresponding to two specified pressure drops). The difference between the results using mixing length Eq. (35) and Eq. (51) is significant, and may be attributed to the fact that the Buleev mixing length, Eq. (51), is considerably smaller than the present adaptation of the McDonald-Camarata length, Eq. (35), in the corner regions of the duct. These results illustrate the sensitivity of the predictions to the choice of length scale, and perhaps reflect the shortcomings of a turbulence model which requires a priori specification of a length scale for a noncircular duct flow.

ACKNOWLEDGMENT

During the preparation of the manuscript, the authors have benefited from several discussions with Dr. Peter R. Eiseman.

REFERENCES

1. Orszag, S. A. and M. Israeli: Numerical Simulation of Viscous Incompressible Flows. Annual Reviews in Fluid Mechanics, Vol. 6, M. Van Dyke (Editor), Annual Reviews, Inc., 1974, p. 281.
2. Fromm, J. E.: Practical Investigation of Convective Difference Approximations of Reduced Dispersion. Physics of Fluids Supplement II, 1969, p. II-3.
3. Morton, K. W.: Stability and Convergence in Fluid Flow Problems. Proc. Roy. Soc. London A, Vol. 323, 1971, p. 237.
4. Douglas, J. and J. E. Gunn: A General Formulation of Alternating Direction Methods. Numerische Math., Vol. 6, 1964, p. 428.
5. Chorin, A. J.: Numerical Study of Thermal Convection in a Fluid Layer Heated from Below. AEC R&D Report TID-4500 (also, New York Univ. Report NYO-1480-61), 1966.
6. Pearson, C. E.: A Computational Method for Viscous Flow Problems. J. Fluid Mech., Vol. 21, 1965, p. 611.
7. Chorin, A. J.: Numerical Solution of the Navier-Stokes Equations. Math. Comp., Vol. 22, 1968, p. 745.
8. Harlow, F. H. and A. A. Amsden: A Numerical Fluid Dynamics Calculation Method for all Flow Speeds. J. Comp. Physics, Vol. 8, 1971, p. 197.
9. Baum, E. and E. Ndefo: A Temporal ADI Computational Technique. Proc. AIAA Computational Fluid Dynamics Conference; AIAA, New York, 1973, p. 133.
10. Peaceman, D. W. and H. H. Rachford: The Numerical Solution of Parabolic and Elliptic Differential Equations. J. Soc. Indust. Appl. Math., Vol. 3, 1955, p. 28.
11. McDonald, H. and W. R. Briley: Three-Dimensional Supersonic Flow of a Viscous or Inviscid Gas. J. Comp. Physics, Vol. 19, 1975, p. 150.
12. Briley, W. R. and H. McDonald: An Implicit Numerical Method for the Multi-dimensional Compressible Navier-Stokes Equations. United Aircraft Research Laboratories Report M911363-6, 1973.

13. Beam, R. M. and R. F. Warming: An Implicit Finite-Difference Algorithm for Hyperbolic Systems in Conservation-Law Form. NASA-Ames Research Center, Note in preparation, 1975.
14. Mitchell, A. R.: Computational Methods in Partial Differential Equations. John Wiley & Sons, Inc., New York, New York, 1969.
15. Ames, W. F.: Numerical Methods for Partial Differential Equations. Barnes & Noble, Inc., New York, New York, 1969.
16. von Rosenberg, D. A.: Methods for the Numerical Solution of Partial Differential Equations. American Elsevier Publishing Co., Inc., New York, New York, 1969.
17. Douglas, J. and B. F. Jones: On Predictor-Corrector Methods for Nonlinear Parabolic Differential Equations. J. Soc. Indust. Appl. Math., Vol. 11, 1963, p. 195.
18. Gourlay, A. R. and J. Ll. Morris: Finite-Difference Methods for Nonlinear Hyperbolic Systems. Math. Comp., Vol. 22, 1968, p. 28.
19. Richtmyer, R. D. and K. W. Morton: Difference Methods for Initial Value Problems. Second Edition. Interscience Publishers, New York, New York, 1967.
20. Bellman, R. E. and R. E. Kalaba: Quasilinearization and Nonlinear Boundary-Value Problems. American Elsevier Publ. Co., Inc., New York, 1965.
21. Douglas, J.: On the Numerical Integration of $u_{xx} + u_{yy} = u_t$ by Implicit Methods. J. Soc. Indust. Appl. Math., Vol. 3, 1955, p. 42.
22. Yanenko, N. N.: The Method of Fractional Steps, Translation Edited by M. Holt. Springer-Verlag, New York, New York, 1971
23. Isaacson, E. and H. B. Keller: Analysis of Numerical Methods. John Wiley & Sons, Inc., New York, New York, 1966.
24. MacCormack, R. W. and A. J. Paullay: Computational Efficiency Achieved by Time Splitting of Finite Difference Operators. AIAA Paper No. 72-154, 1972.
25. Roberts, G. O.: Computational Meshes for Boundary Layer Problems. Proceedings of the Second International Conference on Numerical Methods in Fluid Dynamics, Springer-Verlag, New York, New York, 1971, p. 171.
26. von Mises, R.: On Some Topics in the Fundamentals of Fluid Flow Theory. Proceedings of the 1st U. S. National Congress of Applied Mechanics, ASME, 1951, p. 667.

27. Roache, P. J.: Computational Fluid Dynamics. Hermosa Publishers, Albuquerque, New Mexico, 1972.
28. Spalding, D. B.: A Novel Finite Difference Formulation for Differential Expressions Involving Both First and Second Derivatives. *International Journal for Numerical Methods in Engineering*, Vol. 4, 1972, p. 551.
29. Shapiro, A. S.: *The Dynamics and Thermodynamics of Compressible Fluid Flow*. Vol. I, Ronald Press Co., New York, New York, 1953, p. 162.
30. Beavers, G. S., E. M. Sparrow, and R. A. Magnuson: Experiments on Hydrodynamically Developing Flow in Rectangular Ducts of Arbitrary Aspect Ratio. *Int. J. Heat and Mass Transfer*, Vol. 13, 1970, p. 689.
31. Birkhoff, G., Varga, R. S., and D. Young: Alternating Direction Implicit Methods. *Advances in Computers*. Vol. 3, Academic Press, New York, 1962.
32. Ahmed, S. and E. Brundrett: Turbulent Flow in Noncircular Ducts, Part 1, Mean Flow Properties in the Developing Region of a Square Duct. *Int. J. Heat and Mass Transfer*, Vol. 14, 1971, p. 365.
33. Launder, B. E. and W. M. Ying: Prediction of Flow and Heat Transfer in Ducts of Square Cross Section. *Proc. Instn. Mech. Engrs.*, Vol. 187, 1973, p. 455.
34. Launder, B. E. and D. B. Spalding: Mathematical Models of Turbulence. Academic Press, London, 1972.
35. Hinze, J. O.: Turbulence. McGraw-Hill, New York, 1959, p. 20.
36. McDonald, H. and F. J. Camarata: An extended Mixing Length Approach for Computing the Turbulent Boundary Layer Development. In *Proceedings, Stanford Conference on Computation of Turbulent Boundary Layers*, 1968, p. 83.
37. Schlichting, H.: Boundary-Layer Theory, Sixth Edition, McGraw-Hill, New York, 1968, p. 569.
38. Brundrett, E. and W. D. Baines: Production and Diffusion of Vorticity in Duct Flow. *J. Fluid Mech.*, Vol. 19, 1964, p. 375.
39. Hanjalic, K. and B. E. Launder: A Reynolds Stress Model of Turbulence and Its Application to Thin Shear Flows. *J. Fluid Mech.*, Vol. 52, p. 609.
40. Rotta, J.: Statistische Theorie nichthomogener Turbulenz. *Z. Phys.*, Vol. 129, 1951, p. 547.

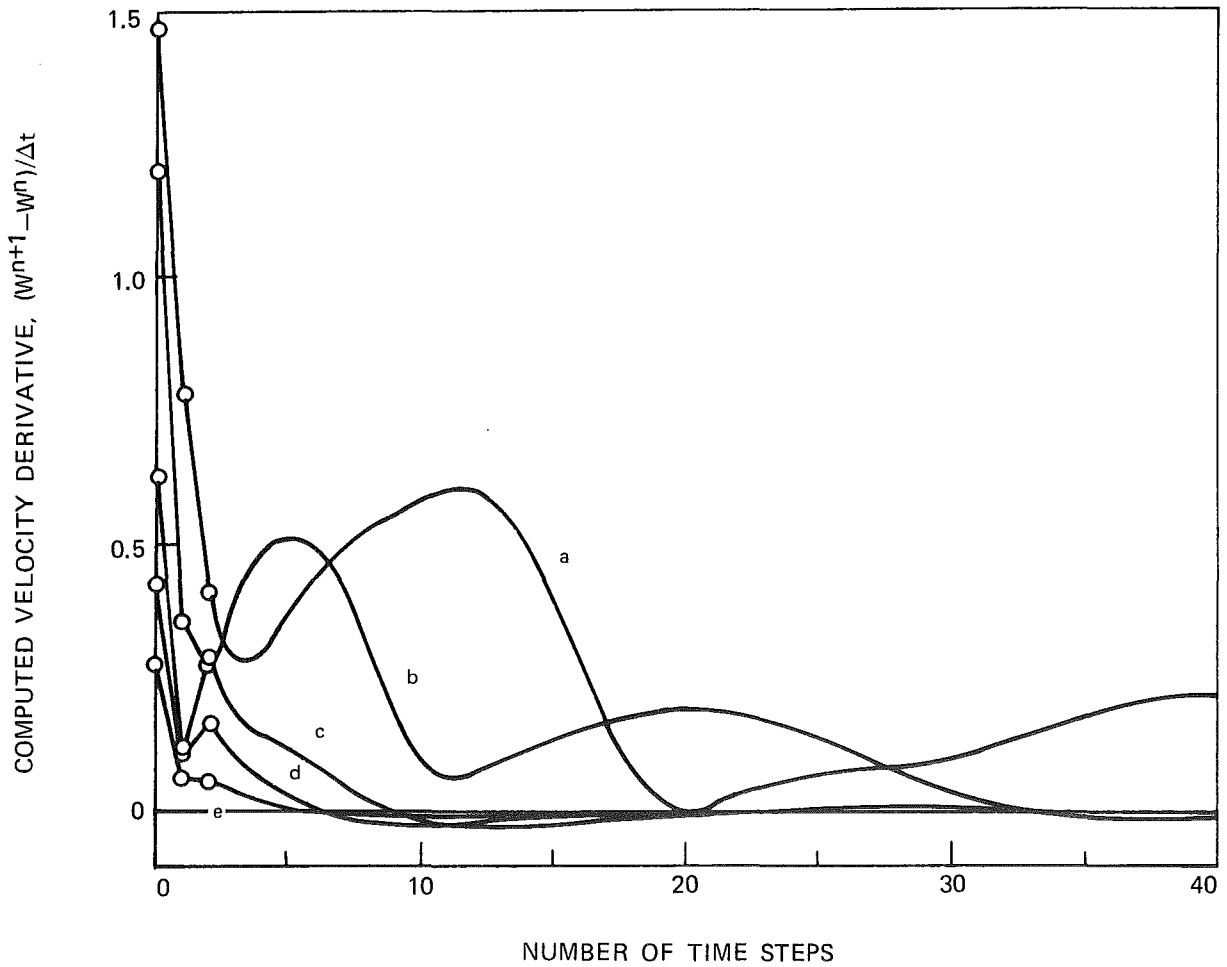
R75-911363-15

41. Buleev, N. I.: Theoretical Model of the Mechanisms of Turbulent Exchange in Fluid Flow. Atomic Energy Research Establishment (U.K.), Translation 957, 1963.
42. Walz, A.: Boundary Layers of Flow and Temperature. M.I.T. Press, Cambridge, Mass., 1969, p. 115.

TRANSIENT BEHAVIOR OF VELOCITY TIME DERIVATIVE AT DOWNSTREAM CENTERLINE
FOR DIFFERENT TIME STEPS

M = 0.44, Re = 60

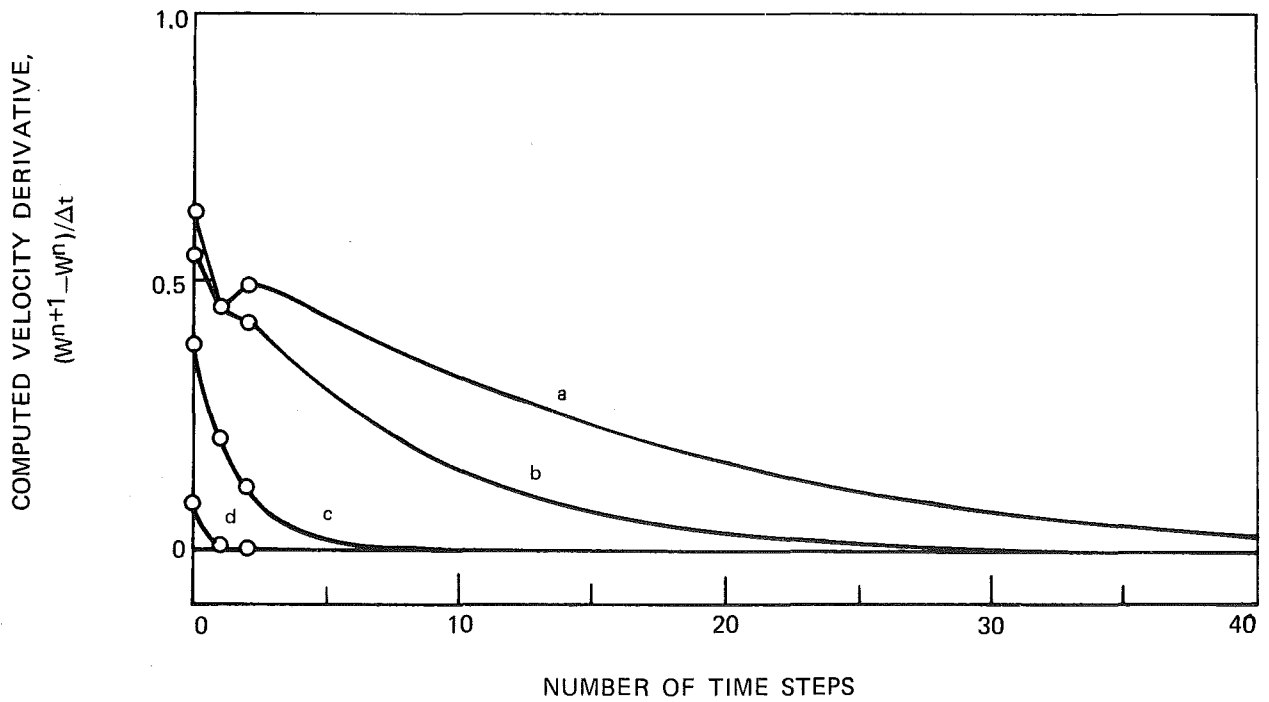
	N_{CFL}	N_{μ}
a -	1.1	0.1
b -	2.2	0.2
c -	10.8	1.1
d -	21.6	2.2
e -	43.2	4.4



TRANSIENT BEHAVIOR OF VELOCITY TIME DERIVATIVE AT DOWNSTREAM CENTERLINE
FOR DIFFERENT TIME STEPS

M = 0.044, Re = 60

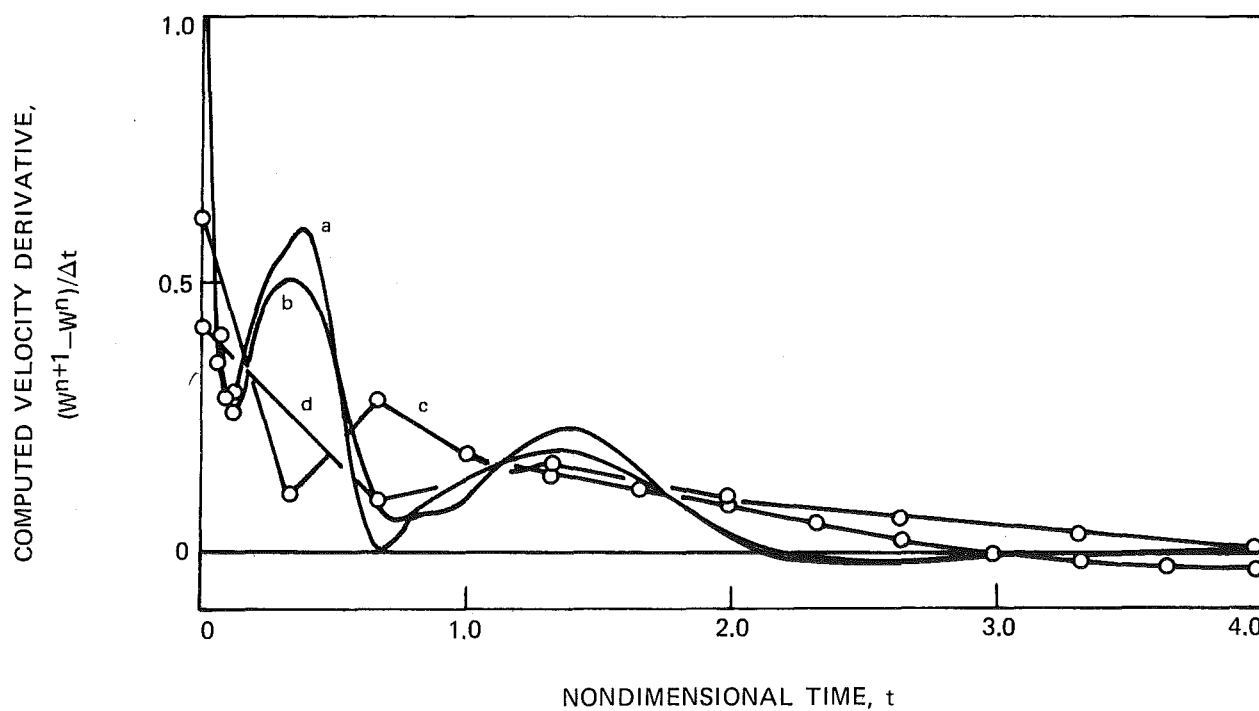
	N_{CFL}	N_{μ}
a -	14.7	0.2
b -	29.4	1.0
c -	147.1	2.1
d -	1471	20.6



TRANSIENT BEHAVIOR OF VELOCITY TIME DERIVATIVE AT DOWNSTREAM
CENTERLINE FOR DIFFERENT TIME STEPS

M = 0.44, Re = 60

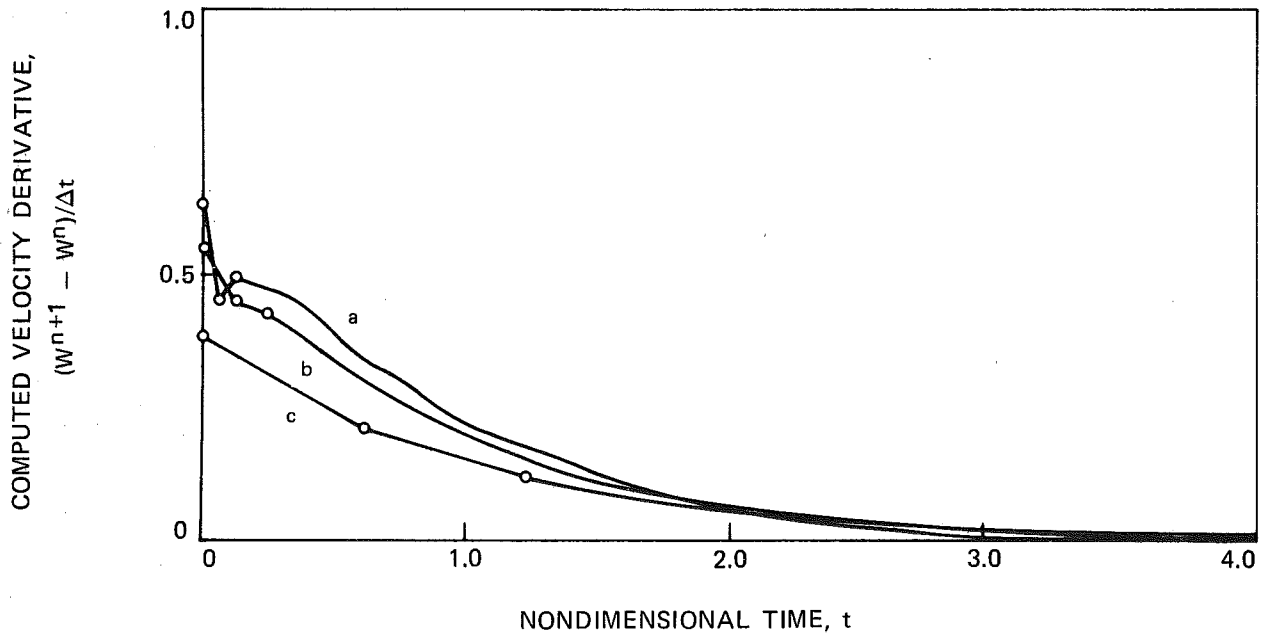
	N_{CFL}	N_{μ}
a -	1.1	0.1
b -	2.2	0.2
c -	10.8	1.1
d -	21.6	2.2



TRANSIENT BEHAVIOR OF VELOCITY TIME DERIVATIVE AT DOWNSTREAM CENTERLINE
FOR DIFFERENT TIME STEPS

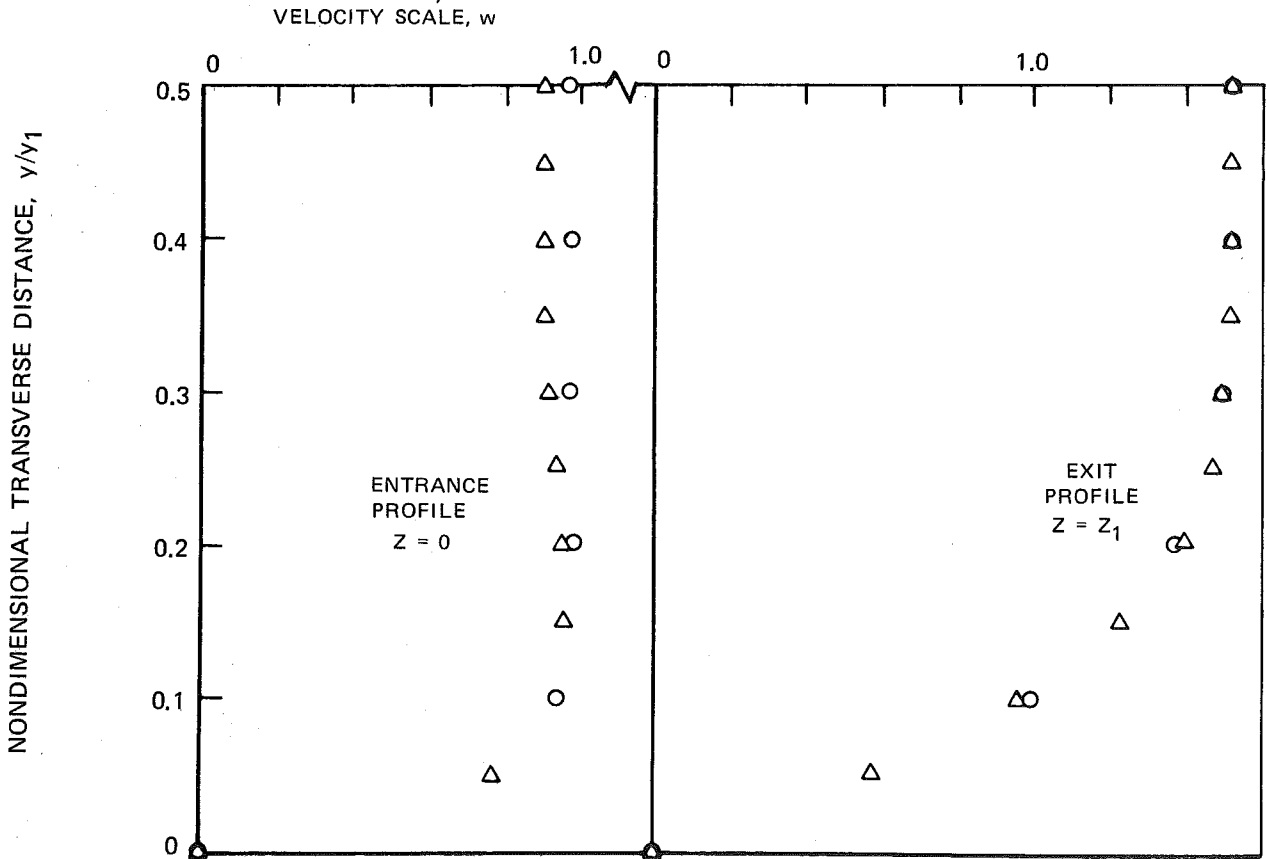
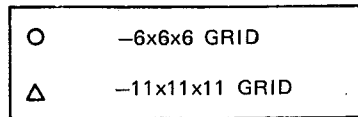
M = 0.044, Re = 60

	N_{CFL}	N_U
a -	14.7	0.2
b -	29.4	1.0
c -	147.1	2.1



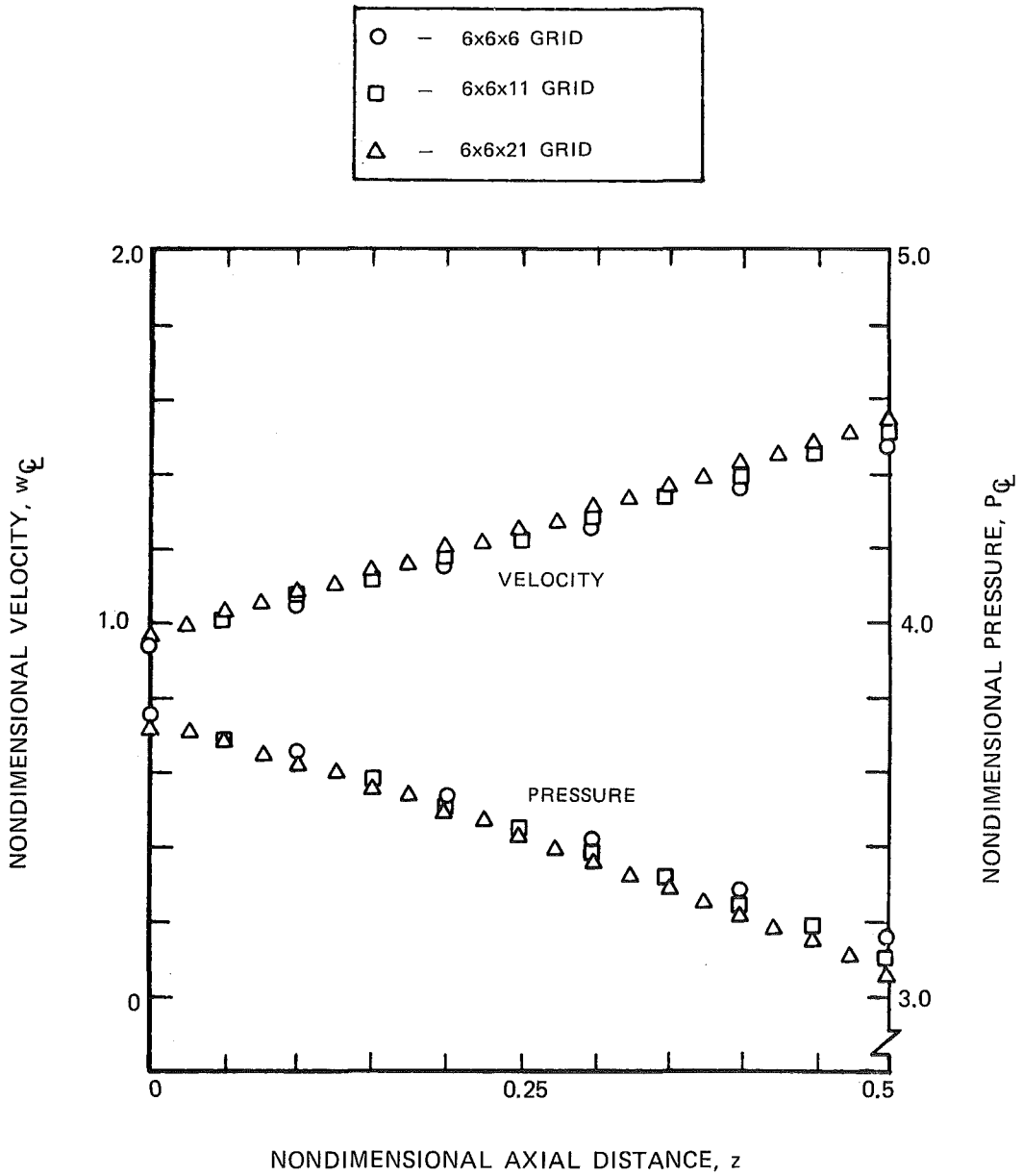
EFFECT OF MESH SIZE ON COMPUTED AXIAL VELOCITY PROFILES AT $x/x_1 = 0.5$

$M = 0.44, Re = 60$



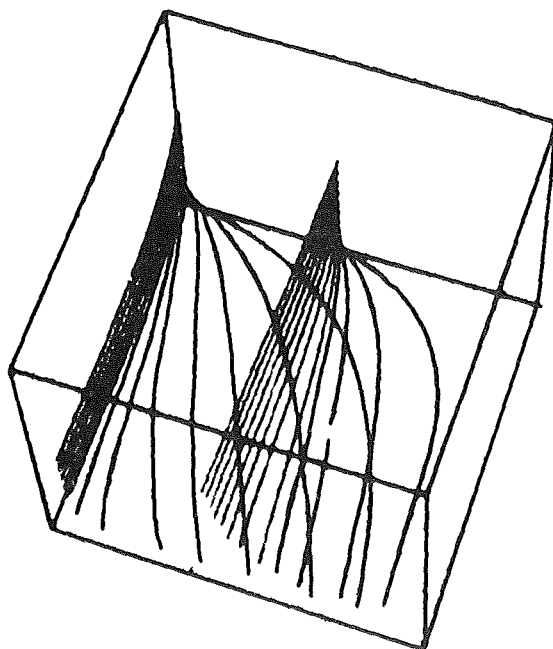
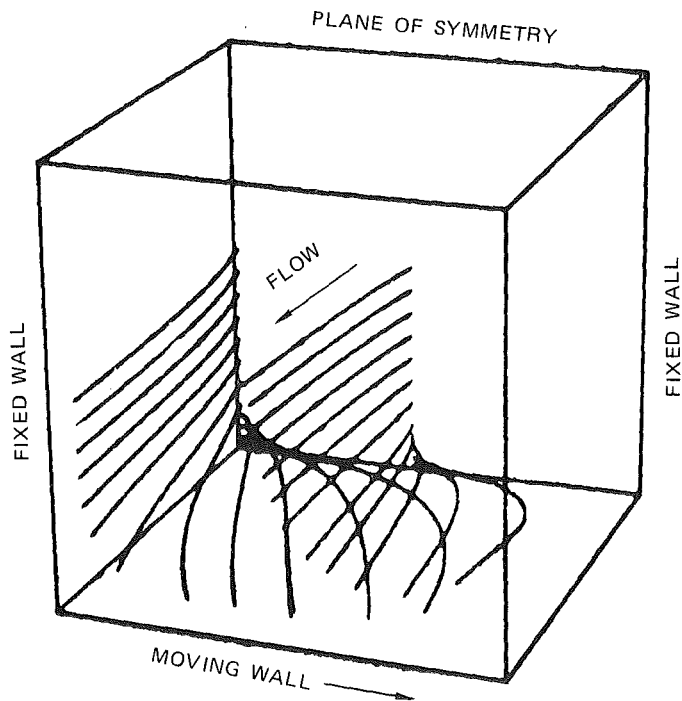
EFFECT OF AXIAL MESH SIZE ON COMPUTED CENTERLINE VELOCITY AND PRESSURE

$M = 0.44, Re = 60$



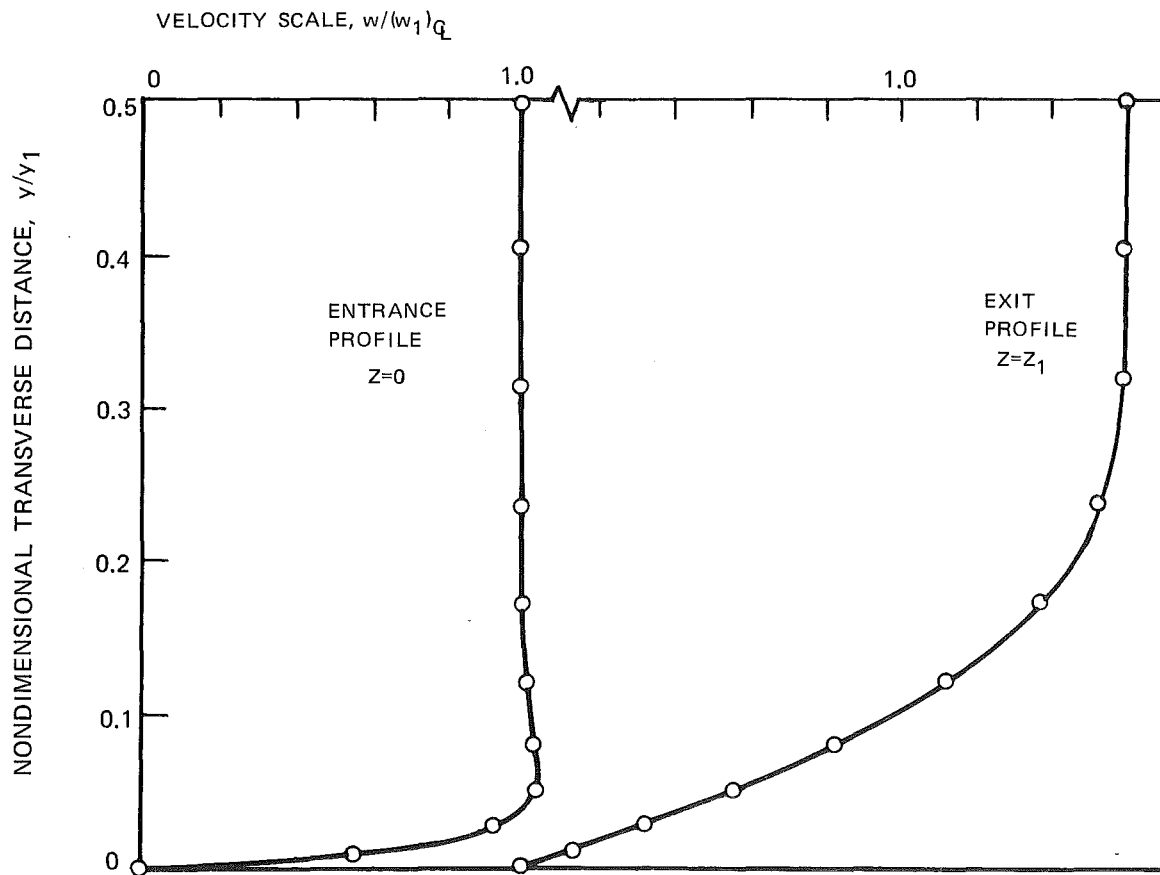
SELECTED STREAMLINES FOR DUCT FLOW WITH MOVING WALLS

$M = 0.44, Re = 60$



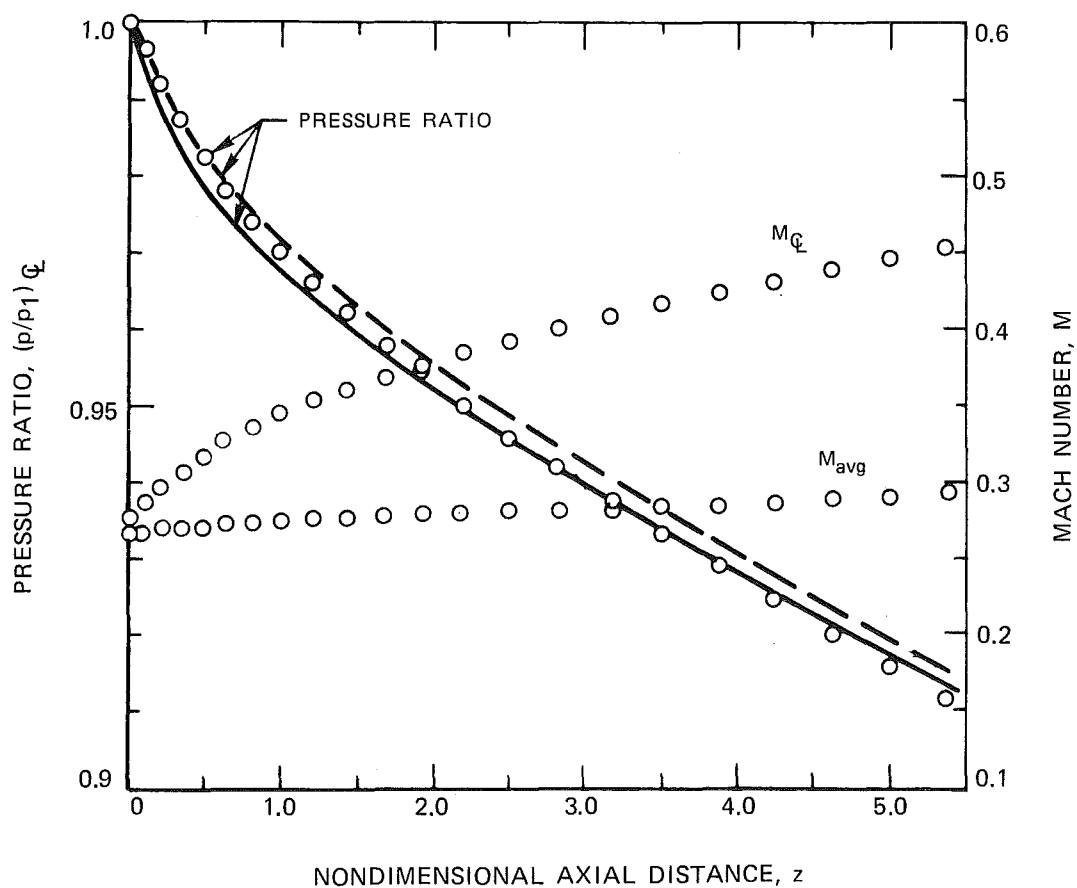
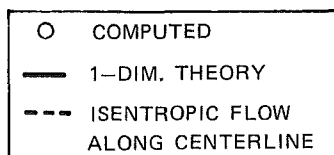
COMPUTED AXIAL VELOCITY PROFILES AT $x/x_1 = 0.5$

$M = 0.3, Re = 600$



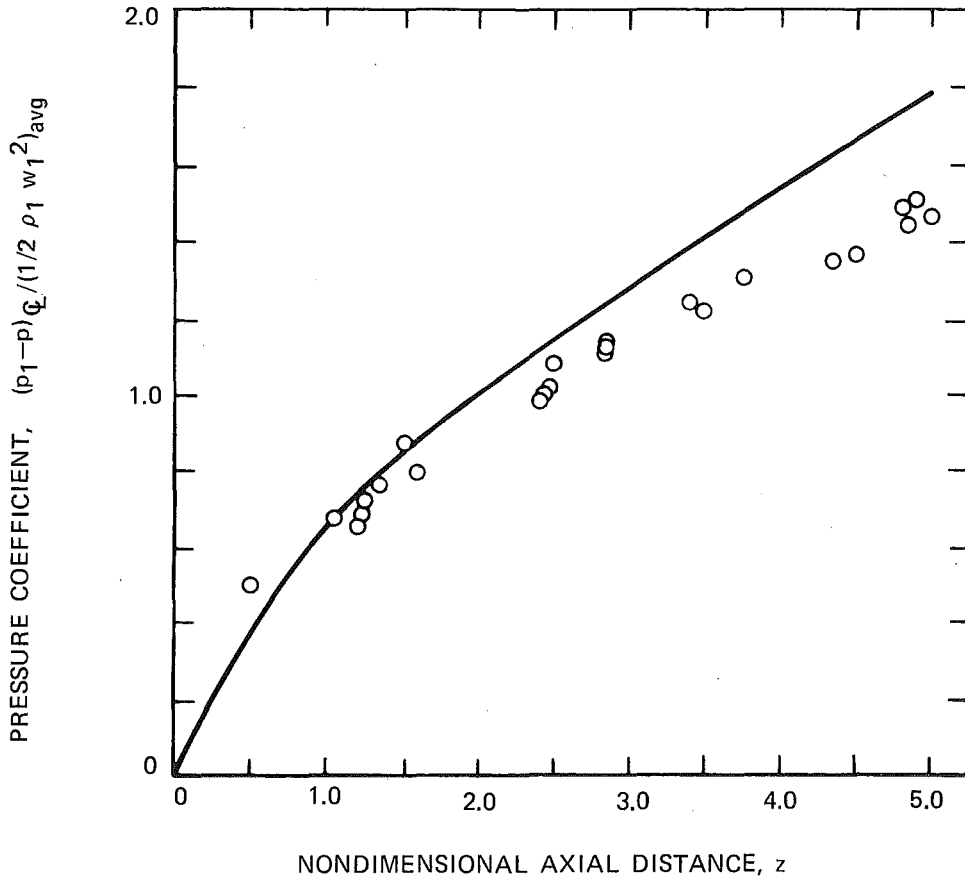
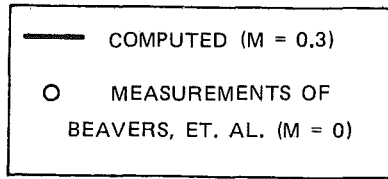
AXIAL VARIATION OF PRESSURE RATIO AND MACH NUMBER

$M = 0.3, Re = 600$

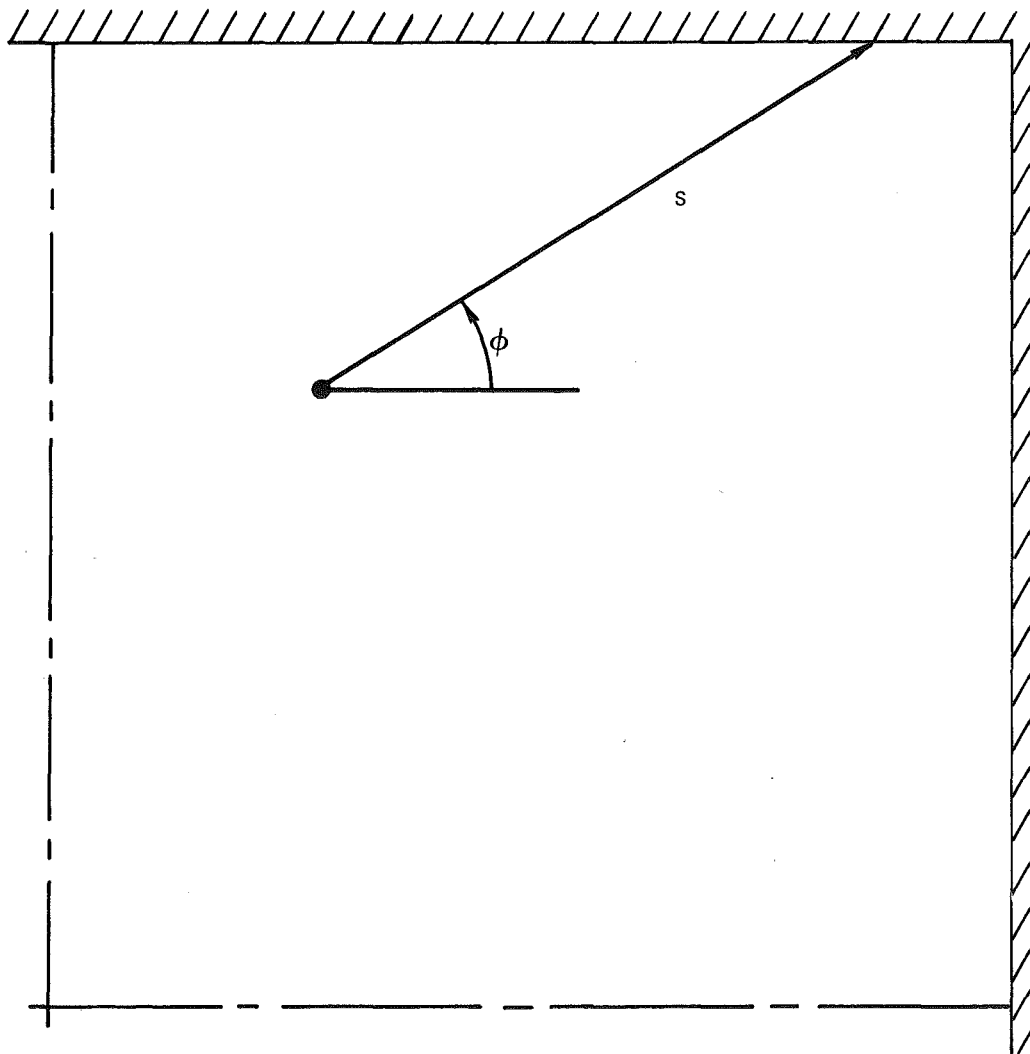


COMPARISON OF COMPUTED AND MEASURED AXIAL PRESSURE DROP

$M = 0.3, Re = 600$



NOTATION FOR CALCULATING BULEEV LENGTH SCALE

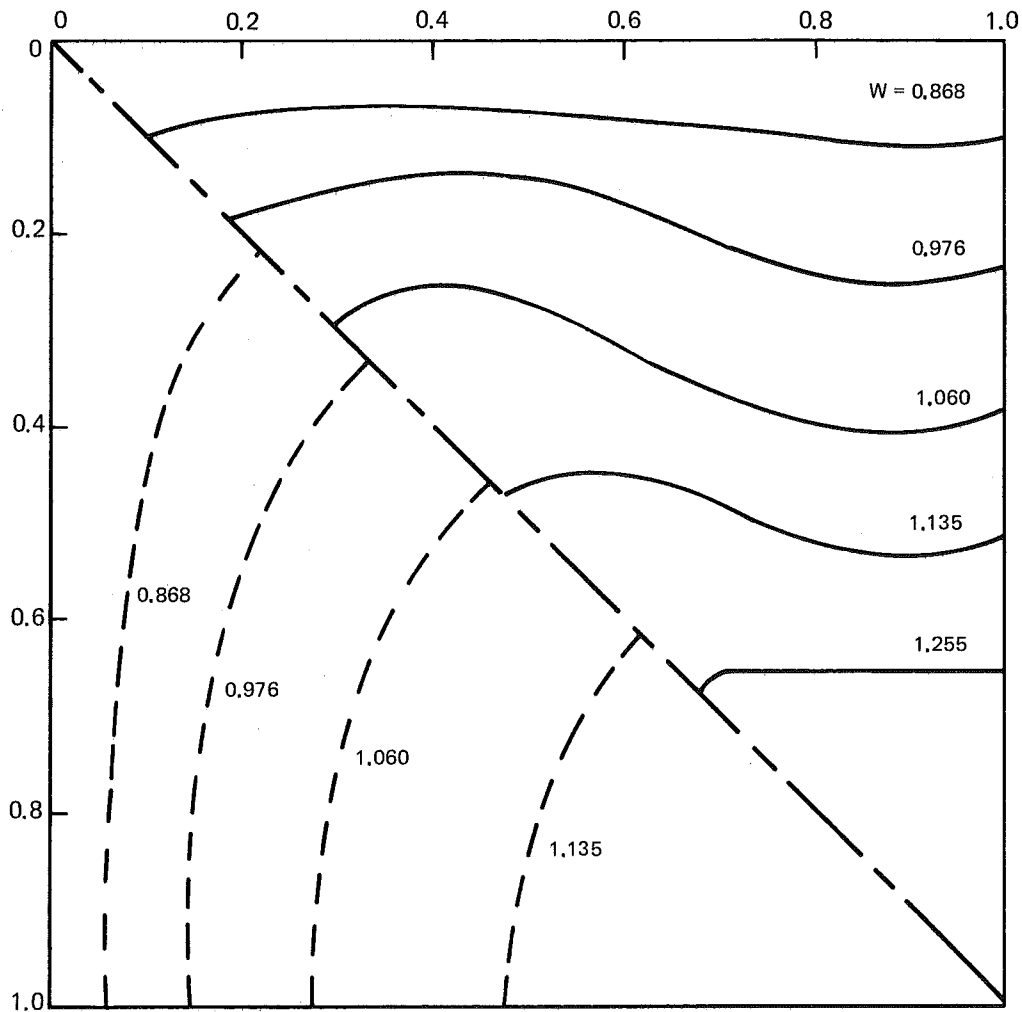


AXIAL VELOCITY CONTOURS FOR FULLY DEVELOPED TURBULENT FLOW IN A SQUARE DUCT

$U_r = 14.63 \text{ M/SEC}$

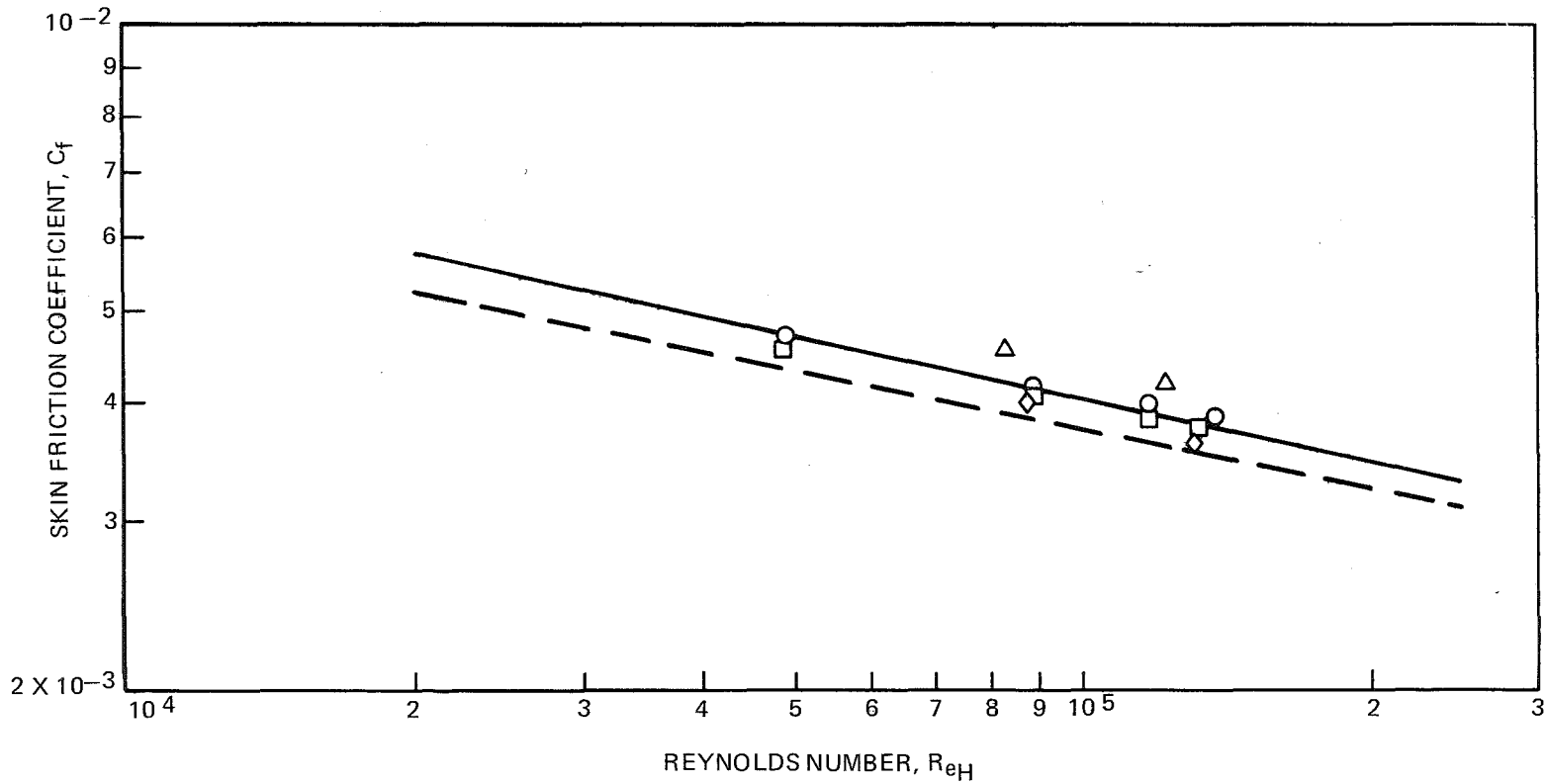
— EXPERIMENT, AHMED AND BRUNDRETT (REF. 32)

- - - PRESENT CALCULATIONS WITHOUT SECONDARY FLOW



COMPARISON OF COMPUTED AND EXPERIMENTAL VALUES OF SKIN FRICTION COEFFICIENT

- | | | |
|---|--|--|
| <ul style="list-style-type: none"> ○ PRESTON TUBE □ DEDUCED FROM $\partial p / \partial z$ △ l FROM EQ. (35) ◇ l FROM EQ. (51) | <ul style="list-style-type: none"> } } } } | <ul style="list-style-type: none"> MEASUREMENTS OF AHMED AND BRUNDRETT (REF. 32) PRESENT CALCULATIONS WITHOUT SECONDARY FLOW |
| <ul style="list-style-type: none"> — WITH SECONDARY FLOW - - - WITHOUT SECONDARY FLOW | <ul style="list-style-type: none"> } } | <ul style="list-style-type: none"> PREDICTIONS OF LAUNDER AND YING (REF. 33) |



APPENDIX

Terms in the governing equation (3) are arranged for application of the numerical method as follows:

$$H^T = (\rho, \rho u, \rho v, \rho w, \rho T) \quad (A-1)$$

$$\mathcal{D}_x(\phi) = \begin{pmatrix} -\partial(\rho u)/\partial x \\ -\partial(\rho u^2 + \rho T/\gamma M^2)/\partial x + \partial^2(u/Re)/\partial x^2 \\ -\partial(\rho uv)/\partial x + \partial^2(v/Re)/\partial x^2 \\ -\partial(\rho uw)/\partial x + \partial^2(w/Re)/\partial x^2 \\ -\partial(\rho uT)/\partial x + (1-\gamma)\rho T \partial u/\partial x + \partial^2(\gamma T/Re Pr)/\partial x^2 \end{pmatrix} \quad (A-2)$$

$$\mathcal{D}_y(\phi) = \begin{pmatrix} -\partial(\rho v)/\partial y \\ -\partial(\rho uv)/\partial y + \partial^2(u/Re)/\partial y^2 \\ -\partial(\rho v^2 + \rho T/\gamma M^2)/\partial y + \partial^2(v/Re)/\partial y^2 \\ -\partial(\rho vw)/\partial y + \partial^2(w/Re)/\partial y^2 \\ -\partial(\rho vT)/\partial y + (1-\gamma)\rho T \partial v/\partial y + \partial^2(\gamma T/Re Pr)/\partial y^2 \end{pmatrix} \quad (A-3)$$

$$\mathcal{D}_z(\phi) = \begin{pmatrix} -\partial(\rho w)/\partial z \\ -\partial(\rho u w)/\partial z + \partial^2(u/Re)/\partial z^2 \\ -\partial(\rho v w)/\partial z + \partial^2(v/Re)/\partial z^2 \\ -\partial(\rho w^2 + \rho T/\gamma M^2)/\partial z + \partial^2(w/Re)/\partial z^2 \\ -\partial(\rho w T)/\partial z + (1-\gamma)\rho T \partial w/\partial z + \partial^2(\gamma T/Re Pr)/\partial z^2 \end{pmatrix} \quad (A-4)$$

$$S^T = \left(0, \frac{1}{3Re} \frac{\partial(\nabla \cdot U)}{\partial x}, \frac{1}{3Re} \frac{\partial(\nabla \cdot U)}{\partial y}, \frac{1}{3Re} \frac{\partial(\nabla \cdot U)}{\partial z}, \gamma(\gamma-1) M^2 \Phi / Re \right) \quad (A-5)$$

UNCLASSIFIED

SECURITY CLASSIFICATION OF THIS PAGE (When Data Entered)

REPORT DOCUMENTATION PAGE		READ INSTRUCTIONS BEFORE COMPLETING FORM
1. REPORT NUMBER R76-911363-15	2. GOVT ACCESSION NO.	3. RECIPIENT'S CATALOG NUMBER
4. TITLE (and Subtitle) SOLUTION OF THE MULTIDIMENSIONAL COMPRESSIBLE NAVIER-STOKES EQUATIONS BY A GENERALIZED IMPLICIT METHOD		5. TYPE OF REPORT & PERIOD COVERED Final Report March 1972 - December 1975
7. AUTHOR(s) W. R. Briley H. McDonald H. J. Gibeling		6. PERFORMING ORG. REPORT NUMBER UTRC Report R76-911363-15
9. PERFORMING ORGANIZATION NAME AND ADDRESS United Technologies Research Center East Hartford, Connecticut 06108		8. CONTRACT OR GRANT NUMBER(s) N00014-72-C-0183
11. CONTROLLING OFFICE NAME AND ADDRESS		10. PROGRAM ELEMENT, PROJECT, TASK AREA & WORK UNIT NUMBERS NR 061-202
14. MONITORING AGENCY NAME & ADDRESS (if different from Controlling Office) Office of Naval Research Arlington, VA 21217		12. REPORT DATE January 1976
		13. NUMBER OF PAGES 60
		15. SECURITY CLASS. (of this report) UNCLASSIFIED
16. DISTRIBUTION STATEMENT (of this Report) Approved for Public Release; distribution unlimited		15a. DECLASSIFICATION/DOWNGRADING SCHEDULE
17. DISTRIBUTION STATEMENT (of the abstract entered in Block 20, if different from Report)		
18. SUPPLEMENTARY NOTES		
19. KEY WORDS (Continue on reverse side if necessary and identify by block number) 1 Implicit Numerical Method 2 Navier-Stokes Equations Compressible Flow Linearization		
20. ABSTRACT (Continue on reverse side if necessary and identify by block number) In an effort to exploit the favorable stability properties of implicit methods and thereby increase computational efficiency by taking large time steps, an implicit finite-difference method for the multidimensional Navier-Stokes equations is presented. The method consists of a generalized implicit scheme which has been linearized by Taylor expansion about the solution at the known time level to produce a set of coupled linear difference equations which		

UNCLASSIFIED

SECURITY CLASSIFICATION OF THIS PAGE(When Data Entered)

are valid for a given time step. To solve these difference equations, the Douglas-Gunn procedure for generating alternating-direction implicit (ADI) schemes as perturbations of fundamental implicit difference schemes is employed. The resulting sequence of narrow block-banded systems can be solved efficiently by standard block-elimination methods. The method is a one-step method, as opposed to a predictor-corrector method, and requires no iteration to compute the solution for a single time step. The use of both second and fourth order spatial differencing is discussed. Test calculations are presented for a three-dimensional application to subsonic flow in a straight duct with rectangular cross section. Stability is demonstrated for time steps which are orders of magnitude larger than the maximum allowable time step for conditionally stable methods as determined by the well known CFL condition. The computational effort per time step is discussed and is very approximately only twice that of most explicit methods. The accuracy of computed solutions is examined by mesh refinement and comparison with other analytical and experimental results. Finally, some test calculations for turbulent flow were made using a simple turbulence model consisting of an eddy viscosity and specified mixing length. The results of these calculations are discussed.

SECURITY CLASSIFICATION OF THIS PAGE(When Data Entered)